An anionic, chelating C(sp 3) / NHC ligand from the combination of N-heterobicyclic carbene and barbituric heterocycle

Idir Benaissa, Katarzyna Gajda, Laure Vendier, Noël Lugan, Anna Kajetanowicz, Karol Grela, Véronique Michelet, Vincent César, Stéphanie Bastin

▶ **To cite this version:**

Idir Benaissa, Katarzyna Gajda, Laure Vendier, Noël Lugan, Anna Kajetanowicz, et al.. An anionic, chelating C(sp 3) / NHC ligand from the combination of N-heterobicyclic carbene and barbituric heterocycle. Organometallics, 2021, 40 (18), pp.3223-3234. 10.1021/acs.organomet.1c00458 . hal-03356487

HAL Id: hal-03356487
https://hal.science/hal-03356487v1

Submitted on 28 Sep 2021

HAL is a multi-disciplinary open access archive for the deposit and dissemination of scientific research documents, whether they are published or not. The documents may come from teaching and research institutions in France or abroad, or from public or private research centers.

L'archive ouverte pluridisciplinaire **HAL**, est destinée au dépôt et à la diffusion de documents scientifiques de niveau recherche, publiés ou non, émanant des établissements d'enseignement et de recherche français ou étrangers, des laboratoires publics ou privés.

An anionic, chelating *C*(sp^3) / NHC ligand from the combination of *N*-heterobicyclic carbene and barbituric heterocycle

Idir Benaissa,[†] Katarzyna Gajda,[†,‡] Laure Vendier,[†] Noël Lugan,[†] Anna Kajetanowicz,[‡] Karol Grela,[‡] Véronique Michelet,[§] Vincent César,[†,*] Stéphanie Bastin[†,*]

[†] LCC-CNRS, Université de Toulouse, CNRS, 205 route de Narbonne, 31077 Toulouse Cedex 4, France

[‡] Faculty of Chemistry, Biological and Chemical Research Centre, University of Warsaw, Żwirki i Wigury 101, 02-089 Warsaw, Poland

[§] University Côte d'Azur, Institut de Chimie de Nice, UMR 7272 CNRS Parc Valrose, Faculté des Sciences 06100 Nice, France

ABSTRACT: The coordination chemistry of the anionic NHC **1**$^-$ based on an imidazo[1,5-*a*]pyridin-3-ylidene (IPy) platform substituted at the C5 position by an anionic barbituric heterocycle was studied with d^6 (Ru(II), Mn(I)) and d^8 (Pd(II), Rh(I), Ir(I), Au(III)) transition metal centers. While the anionic barbituric heterocycle is planar in the zwitterionic NHC precursor **1**·H, NMR spectroscopic analyses supplemented by X-Ray diffraction studies evidenced the chelating behavior of ligand **1**$^-$ through the carbenic and the malonic carbon atoms in all complexes, resulting from a deformation of the lateral barbituric heterocycle. The complexes were obtained by reaction of the free carbene with the appropriate metal precursor except for the Au(III) complex **10**, which was obtained by oxidation of the antecedent gold(I) complex [AuCl(**1**)]$^-$ with $PhICl_2$ as an external oxidant. During the course of the process, a kinetic gold(I) intermediate **9** resulting from the oxidation of the malonic carbon of the barbituric moiety was isolated upon crystallization from the reaction mixture. The ν_{CO} stretching frequencies recorded for complex [Rh(**1**)$(CO)_2$] (**5**) demonstrated the strong donating character of the malonate-*C*(sp^3)-NHC ligand **1**$^-$. The ruthenium complex [Ru(**1**)Cl(p-cymene)] (**11**) was implemented as a pre-catalyst in the dehydrogenative synthesis of carboxylic acid derivatives from primary alcohols and exhibited high activities at low catalyst loadings (25-250 ppm) and a large tolerance towards functional groups.

INTRODUCTION

In transition metal chemistry, *N*-Heterocyclic Carbenes (NHCs) have established as one of the most prominent ligand types.[1,2] Their accessibility, synthetic flexibility,[3,4] and the beneficial impact on the stability and catalytic, photophysical, or biological properties of their organometallic complexes are key features that have stimulated research in NHC organometallic chemistry.[5,6,7] Capitalizing on the strong and non-labile character of the metal-carbene bond,[8] the NHC units have served in particular as pivotal, "anchoring" functions in polydentate ligand architectures. The introduction of an additional coordinating function, such as amine, *N*-heterocycle, alcohol, phosphine, or thioether on the N-side arm led to chelating or pincer-type heteroelement-NHC ligands.[9] Alternatively, connecting two or more NHC units led to the well-known poly-NHCs ligand class.[10]

Conversely, the development of anionic, LX-type *C*-NHC ligands has been relatively less explored, especially with a *C*(sp^3) carbon atom as second coordinating unit. A first subclass is constituted by bidentate hydrocarbyl / NHC ligands, in which a cyclometalation occurs on the NHC backbone at the benzylic, or a (primary or secondary) alkyl position as in **A-C** (Figure 1).[11,12,13,14] Due to the high reactivity of the non-stabilized alkyl moiety, these cyclometalated complexes are usually highly sensitive to reagents/substrates.[15] A remarkable exception is shown by the *Z*-selective metathesis catalyst **C**, in which the chelating nature of the NHC ligand is a key feature to achieve the stereoselectivity observed during the reaction. The second sub-class consists of the combination of an NHC unit with a stabilized *C*(sp^3) ligand such as phosphonium ylide (**D**),[16] η^1-fluorenyl (**E**),[17] or α-cyanoalkyl (**F**) moieties (Figure 1).[18]

In the course of our ongoing research program on functionalized NHC ligands,[19] we have previously reported the synthesis of the stable anionic NHC **1**$^-$ consisting of an imidazo[1,5-*a*]pyridin-3-ylidene (IPy)[20] substituted by a pending anionic barbituric unit. We have shown that **1**$^-$ is able to coordinate a gold(I) center through the carbene function only, the lateral anionic heterocycle remaining untouched and eventually available for further derivatization.[21] Indeed, the anionic malonate moiety could be further *O*-functionalized by reaction with electrophiles, opening the way to diversity of ligand structures. As an extension of this work, we report herein a complete study on the coordination behavior of ligand **1**$^-$ toward a series of d^8 (Pd(II), Rh(I), Ir(I), Au(III)) and d^6 (Ru(II), Mn(I)) transition metal centers, demonstrating that **1**$^-$ is also able to act as a stable, chelating and LX-type malonate-*C*(sp^3) / NHC ligand. Such a malonate-derived σ-alkyl ligand is quite rare in the literature,[22,23] and, to the best of our knowledge, has been incorporated only twice as constitutional unit in ancillary ligand.[24]

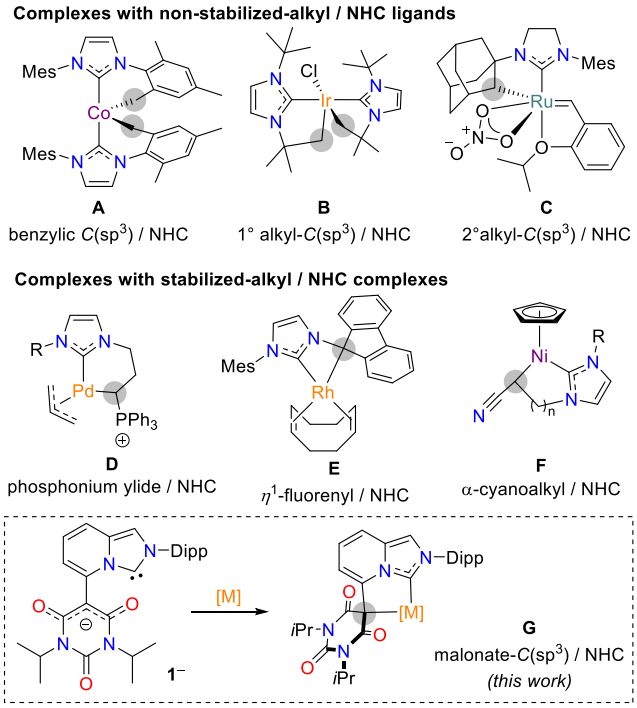

Figure 1. Representative examples of anionic, bidentate *C*(sp^3) / NHC complexes. The coordinating *C*(sp^3) atom is highlighted with a grey sphere. Dipp: 2,6-diisopropylphenyl, Mes: mesityl.

RESULTS AND DISCUSSION

The zwitterionic precursor **1**·H was easily deprotonated at room temperature in THF using a slight excess of lithium bis(trimethylsilyl)amide (LiHMDS) as a strong base, to give the stable free anionic carbene [**1**]Li in quantitative yield (Scheme 1). Its formulation was inferred in particular from its ^{13}C NMR spectrum, the resonance of the N$_2$*C* carbenic carbon atom being observed at δ_C 199.2 ppm.[21] This value is slightly shielded compared to the ones reported in the literature for classical free IPy-type NHCs (206- 209 ppm)[25] and might be indicative of a coordination of the carbene center to the lithium cation.[5b] Treatment of [**1**]Li with 0.5 equivalent of [PdCl(allyl)]$_2$ cleanly led to the formation of the corresponding air and moisture stable [Pd(allyl)(**1**)] complex **2** as a white solid in 75% yield after purification through a column chromatography (Scheme 1). Complex **2** was fully characterized by spectroscopic and analytical methods, which evidenced in particular the coordination of the carbenic and central malonate carbon centers on the Pd(II) center, reflecting a bidentate and chelating coordination mode. This could be deduced from the chemical shift of the NHC carbon atom recorded at δ_C 170.7 ppm in the ^{13}C NMR spectrum, similar to related bidentate [Pd(allyl)(L^IPy)] complexes,[19a, 26] and by the shielding of the central malonic carbon atom from δ_C 88.2 ppm in [**1**]Li to δ_C 66.9 ppm suggesting a partial hybridization change from sp^2 in [**1**]Li to a more-pronounced sp^3 character. We had already observed the same behavior yet with a higher magnitude in a fully-organic 4,6-dioxopyrimidine compounds derived from the anionic *malo*NHC carbene (*malo*NHC = anionic 6-oxo-6*H*-pyrimidin-2-ylidene-4-olate).[27] The molecular structure of complex **2** was then firmly established by a single-crystal X-Ray diffraction (Figure 2 and Table 1) and confirmed the chelating nature of ligand **1**$^-$, with a Pd1-C1 distance of 2.0191(19) Å, in the typical range of Pd-C$_{NHC}$ bond lengths, and a Pd1-C8 distance of 2.2241(18) Å. The latter bond length appears significantly longer than other types of Pd-C(sp^3) bonds in chelating systems previously reported in the literature [2.10-2.17 Å].[16, 22d, 24c, 28] This rather long Pd-C distance associated with the fairly acute bite angle C1-Pd1-C8 of 81.33(7)° and the yaw angle[29] θ of 13.94° reflect the constrained ligand structure in **2**. This significant yaw angle is quite similar to the yaw angles measured in complexes of the related iminophosphorane-IPy ligand, previously reported by us, and originates from the rigidity of the bicyclic imidazopyridine scaffold.[19a] Finally, the noticeable pyramidalization of the malonate carbon (Σ_αC8 = 344.86°) confirms the formulation of ligand **1**$^-$ as an anionic bidentate C(sp^3) / NHC ligand.

Scheme 1. Generation and coordination chemistry of anionic ligand 1$^-$ with d^8 metallic centers. COD: 1,5-cyclooctadiene, NBD: 2,5-norbornadiene.

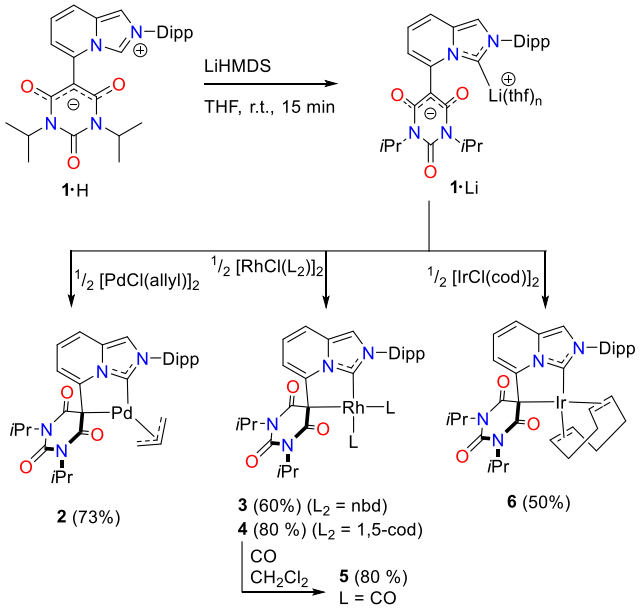

The coordination abilities of ligand **1**$^-$ were further investigated with other d^8 transition metals such as Ir(I) and Rh(I) metallic centers. Reaction of the free NHC **1**·Li with [RhCl(nbd)]$_2$, [RhCl(cod)]$_2$ and [Ir(cod)Cl]$_2$ as metallic precursors afforded the Rh(I) complexes **3** and **4,** and the Ir(I) complex **6** in 60%, 82%, and 51% isolated yields, respectively. All three complexes were stable and could be purified by column chromatography. However, complex **6** appeared to be less stable in solution than its rhodium counterparts as slow de-coordination of the cod ligand was observed during the collection of NMR data. The ^{13}C NMR spectra of Rh(I) complexes **3** and **4** confirmed the chelating nature of ligand **1**$^-$ as both malonic and carbenic carbons resonate as doublets at δ_C 69.8 ppm ($^1J_{C\text{-}Rh}$ = 14.3 Hz) and 68.8 ppm ($^1J_{C\text{-}Rh}$ = 14.4 Hz) for the malonic carbon, and at δ_C 166.8 ppm ($^1J_{C\text{-}Rh}$ = 60.8 Hz) ppm and 165.4 ($^1J_{C\text{-}Rh}$ = 55.2 Hz) ppm for the carbenic carbon in complexes **3** and **4**, respectively (Table 2). The same analysis could be achieved on the Ir(I) complex **6** as the resonances of the carbenic and malonic carbon centers fall into the same range (δ_C 165.8 and 70.6 ppm, respectively).

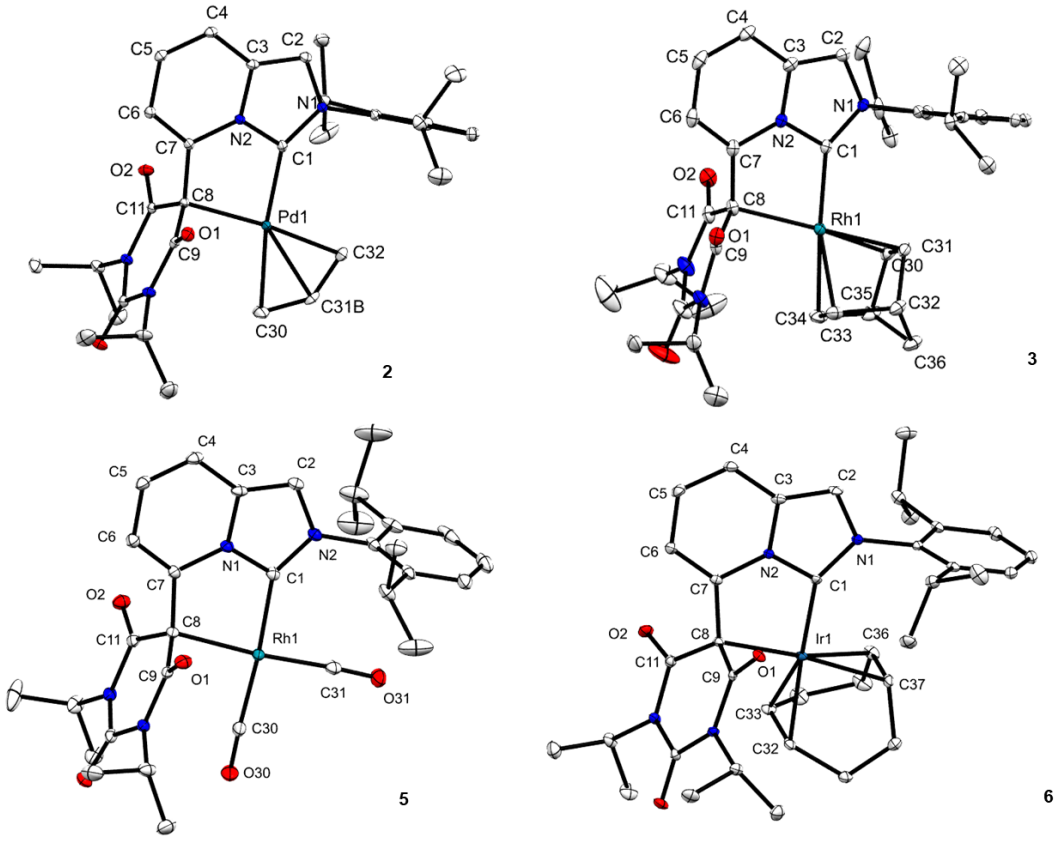

Figure 2. Molecular structures of complexes **2**, **3**, **5**, and **6**. Ellipsoids are drawn at the 30% probability level. Hydrogen atoms have been omitted for clarity. Selected bond lengths and angles are reported in Table 1.

Table 1. Selected bond lengths (Å) and angles (°) for the complexes 2, 3, 5, and 6.

2		**3**		**5**		**6**	
Pd1-C1	2.0191(19)	Rh1-C1	2.014(2)	Rh1-C1	2.0321(18)	Ir1-C1	2.032(3)
Pd1-C8	2.2241(18)	Rh1-C8	2.269(2)	Rh1-C8	2.2281(19)	Ir1-C8	2.232(3)
Pd1-C30	2.181(2)	Rh1-C30	2.139(2)	Rh1-C30	1.899(2)	Ir1-C32	2.174(3)
Pd1-C31B	2.148(6)	Rh1-C31	2.115(2)	Rh1-C31	1.864(2)	Ir1-C33	2.148(4)
Pd1-C32	2.138(2)	Rh1-C33	2.182(2)	C11-O2	1.217(2)	Ir1-C36	2.131(4)
C8-C9	1.463(3)	Rh1-C34	2.209(2)	C9-O1	1.221(2)	Ir1-C37	2.126(4)
C8-C11	1.467(3)			C31-O31	1.134(3)	C32-C33	1.390(6)
C9-O1	1.224(2)			C30-O30	1.134(3)	C36-C37	1.400(6)
C11-O2	1.221(2)						
N1-C1-N2	103.52(16)	N1-C1-N2	102.79(19)	N1-C1-N2	103.50(15)	N1-C1-N2	102.8(3)
C1-Pd1-C8	81.33(7)	C1-Rh1-C8	79.41(9)	C1-Rh1-C8	80.12(7)	C1-Ir1-C8	79.02(13)
Yaw angle θ	13.94	Yaw angle θ	12.70	Yaw angle θ	13.22	Yaw angle θ	14.05
Σ_{α}C8	344.86	Σ_{α}C8	344.80	Σ_{α}C8	341.21	Σ_{α}C8	340.3

θ = [(N1-C1-M)-(N2-C1-M)]/2

Table 2. ^{13}C NMR chemical shifts for the carbenic and central malonic atoms recorded in $CDCl_3$.

Compound	δ($C_{carbene}$) (ppm)	δ(C_{malo}) (ppm)
1·H	127.2	83.3
1·Li[a]	199.2	88.2
[AuCl(**1**)](PPN)[b]	166.9	86.7
2	170.7	66.9
3	166.8 (d, J_{Rh-C} = 60.8 Hz)	69.8 (d, J_{Rh-C} = 14.3 Hz)
4	165.4 (d, J_{Rh-C} = 55.2 Hz)	68.8 (d, J_{Rh-C} = 14.4 Hz)
5	189.0 (d, J_{Rh-C} = 57.9 Hz)	67.3 (d, J_{Rh-C} = 15.8 Hz)
6	165.8	70.6
9	163.9	64.2
10	141.8	67.5
11	165.5	57.1
12	173.0	60.6

[a] In THF-d^8. [b] In CD_2Cl_2.

The molecular structures of complexes **3** and **6** were confirmed by single-crystal X-ray diffraction and both displayed a typical square planar geometry around the metal centers (Figure 2). While the ligand metrics (metal-C_{NHC} and M-$C_{malonate}$ distances, bite and yaw angles) are similar to the ones previously recorded in complex **2** (see Table 1), it is worth to note that the Rh-C_{NBD} and Ir-C_{COD} distances, which are *trans* to the carbene carbon center are longer than the Rh-C_{NBD} and Ir-C_{COD} bond lengths *trans* to the malonate carbon atom, thus reflecting the more pronounced *trans* influence of the carbenic center. In order to evaluate the electronic properties of ligand **1**$^-$ by IR spectroscopy, the dicarbonyl complex [Rh(**1**)$(CO)_2$] complex **5** was synthesized from complex **4** by bubbling CO gas into a solution of complex **4** in dichloromethane. Complex **5** was isolated as an air and moisture stable yellow powder in 80% yield. It was fully characterized by analytical techniques supplemented by an X-ray diffraction analysis (Figure 2). As expected, complex **5** displays a typical square planar geometry around the d^8 Rh(I) metal center. The ν_{CO} values of complex **5** in CH_2Cl_2 solution were recorded at 2010 and 2069 cm^{-1}. Comparison of its average value (ν_{CO}^{av} = 2039 cm^{-1}) with that of the structurally related rhodium complex [**7**](OTf) supported by an IPy-based ligand substituted with an iminophosphorane group in position 5 previously reported by our group (ν_{CO}^{av} = 2046 cm^{-1}) revealed that replacing the neutral iminophosphorane moiety by the anionic η^1-barbituric moiety renders the corresponding ligand more donating (Figure 3).[19a] Moreover, it appears that ligand **1**$^-$ induces about the same overall electronic density on Rh(I) center as the strong electron-donating phosphonium ylide / NHC in [**8**](OTf).[30]

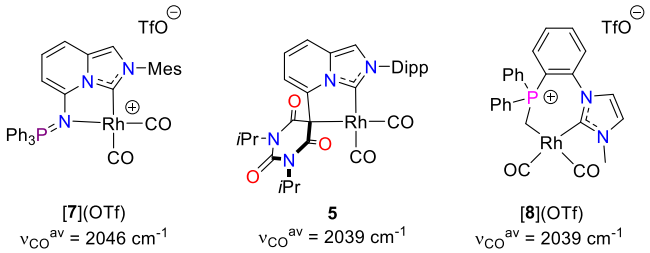

Figure 3. Comparison of the ν_{CO}^{av} stretching frequency values for Rh(I) complexes bearing chelating IPy-iminophosphorane, IPy-barbituric heterocycle, and NHC-phosphonium ylide ligands, respectively.

These results obtained with d^8 metallic centers encouraged us to explore the coordination chemistry of ligand **1**$^-$ with gold(III). Our strategy rested on the oxidation of the gold(I) complex [AuCl(**1**)]Li, previously reported by us, using an external oxidant. Accordingly, [AuCl(**1**)]Li was generated *in situ* by reaction of free carbene **1**·Li with [AuCl(tht)]. After evaporation of the solvent and without further purification, the resulting gold(I) complex was suspended in dichloromethane and reacted with iodobenzene dichloride $PhICl_2$ (Scheme 2). The color of the suspension changed rapidly from dark green to yellow-orange. The ^{1}H NMR analysis of the crude reaction mixture after 20 min of reaction evidenced the formation of two different products in a 3/1 ratio, whose mixture was separated from impurities and by-products by column chromatography.

Scheme 2. Oxidation of complex [AuCl(1)]Li with $PhICl_2$.

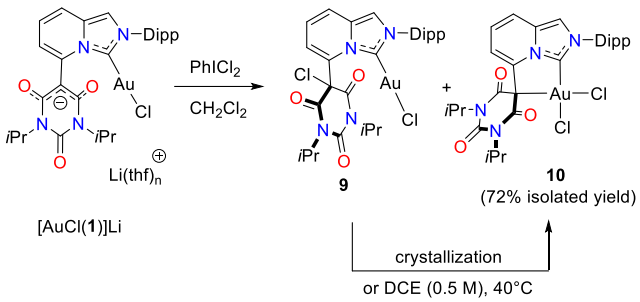

The crystallization of the residue led to dark-green and orange crystals, which were separated manually. The X-ray diffraction analysis of the orange crystals confirmed the formation of the expected Au(III) complex **10** while the analysis of the green crystals evidenced the formation of the Au(I) complex **9**, in which a C-Cl bond has been formed on the central malonic position of the barbituric heterocycle indicating a ligand oxidation (Figure 4, Table 3). Moreover, we noted that successive crystallizations of the mixture by slow evaporation of CH_2Cl_2 at room temperature led to the interconversion of the Au(I) complex **9**, initially the major one, into the Au(III) complex **10**, which could finally be isolated in a pure form in 72% overall yield.

In order to get a better understanding of this interconversion, the evolution of a concentrated solution (0.5 M) of complexes **9** and **10** obtained in an initial ratio **9**/**10** = 3/1 in dichloromethane was monitored by ^{1}H NMR. Aliquots were taken and analyzed in acetone-*d6*. The choice of the NMR solvent was driven by the good separation of the signals at 8.35 ppm and 8.20 ppm assigned to the remote proton on the imidazole ring

in complexes **9** and **10**, respectively. The monitoring evidenced a full conversion of complex **9** into complex **10** after 7.7 days. When performed in DCE (0.5 M) at 40°C, full conversion of complex **9** into complex **10** was obtained in 4.6 days. However, no reliable kinetic conversion could be measured despite numerous attempts. The transformation of **9** into **10** is supposed to occur through an intramolecular, SN_2-type oxidative addition of the malonate-type C-Cl bond onto Au(I) center.[31]

The gold(I) complex **9** displays the typical linear geometry coordination of gold(I) complexes with a C1-Au1-Cl1 angle of 177.64(7)°. Due to the sp^3 hybridization character of the C8 carbon, the barbituric heterocycle is not entirely planar anymore, and the C8 carbon deviates by 0.449 Å from the mean plane formed by the C9-N3-C10-N4-C11 atoms with the chloride pointing in the opposite direction to the metal center. This specific geometry is consistent with an outer-sphere chlorination reaction and forces the two carbon atoms C9 and C11 to be closer to Au1 (Au1-C9 = 3.069 Å and Au1-C11 = 3.065 Å) than in complex [AuCl(**1**)]PPN (3.317 Å and 3.409 Å respectively).[21]

The Au(III) center in complex **10** displays the typical square planar geometry of gold(III) complexes with the ligand **1**$^-$ chelating the metal center through coordination of the sp^3 malonic carbon C8 and the carbenic carbon C1.

Complexes **9** and **10** were fully characterized by ^{1}H and ^{13}C NMR. The ^{1}H NMR spectrum of **10** displays a doublet at 6.73 ($^3J_{C\text{-}H}$ = 6.8 Hz) ppm which corresponds to the proton in position 6 of the IPy bicycle. This signal is significantly shielded compared to its equivalent in the gold(I) complex [AuCl(**1**)]PPN (7.21 ppm), which can be explained by the coordination of the malonic carbon to the gold metallic center. This trend was already noticed in the previous complexes **2**-**6**. Conversely, this proton appears to be deshielded at 7.72 ppm in complex **9** due to the presence of the chlorine atom on the malonic carbon. The ^{1}H and ^{13}C NMR spectra reflect the *C*s-symmetry for both complexes **9** and **10**, in which the IPy bicycle defines the symmetry plane in the molecule. In the ^{13}C NMR spectrum, the chemical shift of the malonic carbon atom is recorded at 67.5 ppm for gold(III) complex **10**, which lies in the same range as the chemical shifts recorded for complexes **2**-**6**.

The bidentate coordination mode of ligand **1**$^-$ is not restricted to d^8 transition metals and was also observed in d^6 metal complexes. Indeed, the reaction between free NHC [**1**]Li with the $[RuCl_2(p\text{-cymene})]_2$ and $[MnBr(CO)_5]$ metal precursors led to complexes **11** and **12** in 77% and 37% yields, respectively (Scheme 3).

Scheme 3. Synthesis of d^6-metal complexes 11 and 12

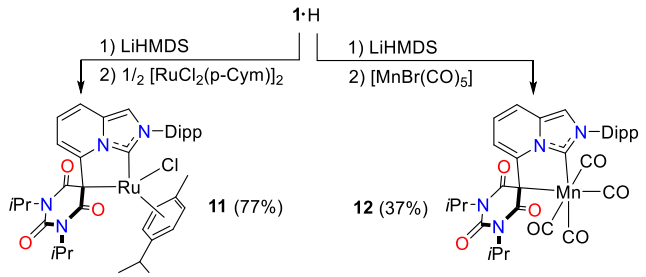

Both complexes were fully characterized by spectroscopic and analytical techniques. In particular, the *C*s-symmetry of the complex **12** is reflected by the presence of three signals in the ^{13}C NMR spectrum corresponding to the four carbonyl ligands: the two peaks at 215.3 ppm and 214.2 ppm are attributed to the carbonyl ligands lying in the plane of the IPy core while the signal at 210.7 ppm corresponds to the two carbonyl ligands on each side of the mirror plane materialized by the IPy bicycle. The molecular structures were firmly confirmed by X-Ray analysis (Figure 4). In both complexes **11** and **12**, the ligand **1**$^-$ displays a κ^2-*C*,*C* bidentate coordination mode with quite acute bite angles of 77.43(17)° and 79.61(6)°, respectively and the highest degrees of sp^3-pyramidalization within the series [Σ_αC8 = 336.1° for **11** and 339.44° for **12**]. The ruthenium complex **11** adopts an half sandwich distorted pseudo-octahedral geometry around the Ru(II) center with the η^6-*p*-cymene occupying three facial coordinating sites and the anionic ligands **1**$^-$ and Cl$^-$ completing the coordination sphere. While the Mn(I) complex **12** displays a distorted octahedral geometry, it is worth to note that the Mn1-C31 and Mn1-C33 bonds [1.8278(16) Å and 1.8230(17) Å, respectively], which are in the coordination plane of ligand **1**$^-$ are significantly shorter than the Mn1-C30 and Mn1-C32 bonds [1.8632(18) Å and 1.8715(17) Å], perpendicular to this plane, due to a stronger backdonation from the Mn center into the π*(CO) orbitals, and evidencing the strong donation of the ligand **1**$^-$.

Reports in the literature showed that ruthenium complexes supported by NHC ligands can promote the dehydrogenative synthesis of carboxylic acids from primary alcohols.[32] More specifically, a highly active catalytic system supported by a cyclometalated κ^2-C,C bidentate NHC ligand was developed by Verpoort and coworkers running at catalyst loading as low as 25 ppm.[33] Based on the typical reaction conditions established by Verpoort, we implemented complex **11** in the aerobic Ru-catalyzed oxidation of benzylic alcohol into benzoic acid starting with 250 ppm of catalyst and 1.2 equiv of KOH in refluxing *o*-xylene (Table 4).

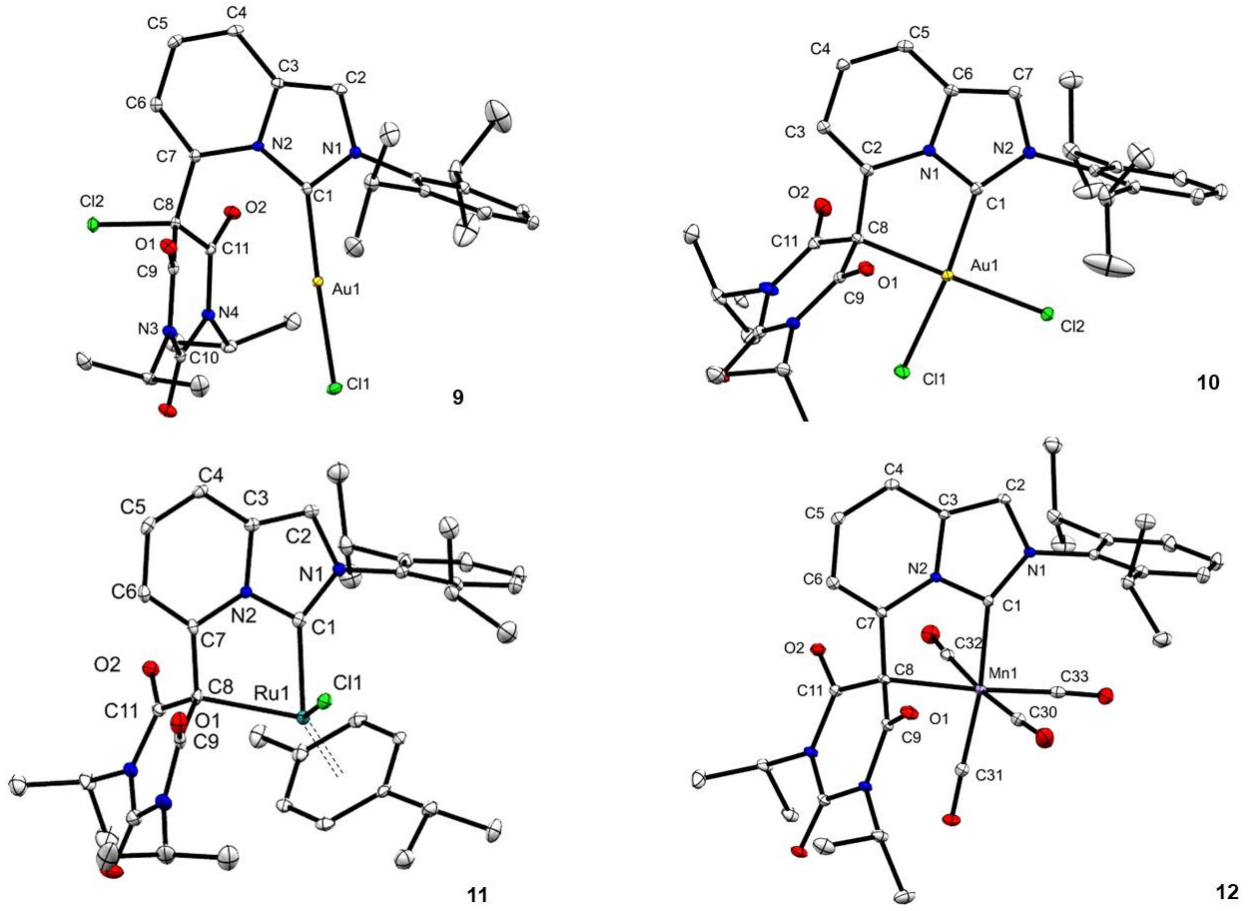

Figure 4. Molecular structures of complexes **9**, **10**, **11**, and **12**. Ellipsoids are drawn at the 30% probability level. Hydrogen atoms have been omitted for clarity. Selected bond lengths and angles are reported in Table 2.

Table 3. Selected bond lengths (Å) and angles (°) for the complexes 9, 10, 11, and 12.

9		10		11		12	
Au1-C1	1.979(2)	Au1-C1	1.9932(19)	Ru1-C1	2.035(4)	Mn1-C1	2.0200(15)
Au1-Cl1	2.2850(6)	Au1-C8	2.1319(19)	Ru1-C8	2.316(4)	Mn1-C8	2.2907(15)
C8-Cl2	1.817(2)	Au1-Cl1	2.3076(5)	Ru1-Cl1	2.3992(12)	Mn1-C30	1.8632(18)
		Au1-Cl2	2.3336(5)			Mn1-C31	1.8278(16)
						Mn1-C32	1.8715(17)
						Mn1-C33	1.8230(17)
N1-C1-N2	104.50(18)	N1-C1-N2	105.03(16)	N1-C1-N2	103.2(4)	N1-C1-N2	103.35(12)
C1-Au1-Cl1	177.64(7)	C1-Au1-C8	82.55(7)	C1-Ru1-C8	77.43(17)	C1-Mn1-C8	79.61(6)
Yaw angle θ	- 6.56	Yaw angle θ	14.10	Yaw angle θ	10.80	Yaw angle θ	12.22
Σ_{α}C8	341.46	Σ_{α}C8	338.21	Σ_{α}C8	336.1	Σ_{α}C8	339.44

θ = [(N1-C1-M)-(N2-C1-M)]/2

Table 4. Ruthenium-catalyzed dehydrogenative oxidation of benzyl alcohol. Optimization of the reaction conditions.[a]

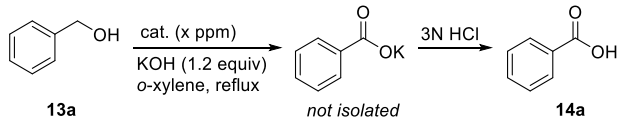

13a *not isolated* **14a**

Entry	Cat. (ppm)	Time (h)	NMR yield (%)[b]	*TON*
1	**11** (250)	2	88[c]	3500
2	**11** (250)	5	96[c]	3800
3	**11** (250)	0.5	36	1400
4	**11** (250)	1	61	2400
5	**11** (250)	1.5	72	2900
6	**11** (250)	2	87	3500
7	**11** (250)	2.5	98	3900
8	**11** (250)	3	>99	>4000
9	**11** (25)	13	65	26000
10	**11** (25)	24	76	30400
11	**11** (10)	24	33	33000
12	**11** (10)	48	73	73000
13	-	5	0.4	
14	$[RuCl_2(p\text{-cym})]_2$ (250)	6	9	180

[a] Typical conditions: benzyl alcohol (7.5 mmol), potassium hydroxide (1.2 equiv), *o*-xylene (1.4 mL) under an open air atmosphere. [b] NMR yields were measured using 1,3,5-trimethoxybenzene as an internal standard. [c] Reaction performed under open argon atmosphere.

The dehydrogenative coupling of benzyl alcohol and potassium hydroxide reaction was first performed under open argon conditions leading to the formation of benzoic acid **14a** in 96% after 5 hours, confirming that molecular dioxygen is not involved in the oxidation process (entry 2). Operating under an open air atmosphere did not alter the activity of the catalyst, as the product **14a** was obtained in 99% yield in only 3 hours (entry 8), highlighting the robustness and the convenient handling of the catalytic system. The subsequent experiments were consequently conducted under aerobic conditions. Oxidation of the benzylic alcohol was successfully performed at a low catalyst loading of 25 and 10 ppm to give **14a** in 76% and 73% yields respectively (entries 10 and 12), leading to a maximum TON of 73000 (entry 12), yet at the expense of longer reaction times. A blank experiment was conducted in the absence of any ruthenium catalyst and traces only of benzoic acid were detected, showing the crucial role of the catalyst and ruling out a possible oxidation of benzylic alcohol under basic aerobic conditions (Entry 13).[34] For the sake of comparison, a second catalytic reaction was set up in the presence of $[RuCl_2(p\text{-cymene})]_2$ dimer leading to very poor yield (9%, entry 14) demonstrating that the activity of the catalytic system relies on the nature of the ligand.

With the optimized conditions in hand (250 ppm of pre-catalyst **11** and 1.2 equiv of KOH in refluxing *o*-xylene for 6 hours), a series of primary alcohols was subjected to the dehydrogenative coupling reaction (Scheme 4). Benzylic alcohols displaying electron-donating groups in *meta* or *para* position **13b-e** were successfully oxidized with good to excellent yields ranging from 83% to 97%, the substitution of the aromatic ring did not alter to a great extent the reaction yields. On the other hand, electron-poor substrates **13g-j** were more reluctant to oxidation and lower yields (46 to 77%) were recorded despite an increase of the catalyst loading (500 ppm for substrates **13g-i**) or longer reaction times (16 h for substrate **13j**). It is worth noting that the oxidation of the halogenated substrates **13g** and **13h** afforded the corresponding acids **14g** and **14h** along with a non-negligible amount of dehalogenated benzoic acid **14a**, this dehalogenation side-reaction being also observed by Verpoort and coworkers.[33] The catalytic system was tolerant to the presence of an acidic function on the aromatic ring, as 4-hydroxybenzyl alcohol **13f** was oxidized to the corresponding carboxylic acid in 49% yield in the presence of 3.3 equiv of KOH. The catalytic system is also compatible with polyaromatic alcohols (**13k**). Next, we investigated the dehydrogenative coupling of aliphatic alcohols **13l-p** with potassium hydroxide. Aliphatic alcohols were successfully oxidized but were less reactive and longer reaction times (16 h) were required to obtain moderate to good yields (46-92%). It is worth noting that the presence of heterocycles did not inhibit the reaction. In particular, 3-pyridylpropionic acid **14m** was isolated in 91% yield, proving the compatibility of the catalytic system with highly coordinating moieties. Introduction of a bulky adamantyl substituent resulted in a drastic decrease of the reaction yield, **14p** being obtained in 31% yield only, to be compared to 92% yield for **14n**. Eventually, the oxidation of hexanol led to hexanoic acid **14o** in a moderate 68% yield. Overall, the efficiency of the present catalytic system based on complex **11** appears quite similar to the reference Verpoort's catalytic system.

CONCLUSION

Through a detailed coordination study, we have shown that the anionic ligand **1**$^-$, composed of an imidazo[1,5-*a*]pyridin-3-ylidene laterally substituted by an anionic barbituric moiety, acts as a chelating, bidentate C_{sp3} / C_{NHC} ligand on square-planar d^8 metallic centers [Pd(II), Rh(I), Ir(I), Au(III)] as well as on (pseudo)octahedral d^6 metallic centers [Ru(II), Mn(I)]. Through the deformation of the barbituric heterocycle and pyramidalization of the central carbon atom of its malonic unit from sp^2 in free **1**·Li to sp^3, the ligand **1**$^-$ afforded stable 5-membered metallacycles, displaying quite acute bite angles [77-82°] and noticeable tilting coordination of the carbenic center [yaw angles: 10-14°] due to the rigidity of its bicyclic scaffold. Most importantly, the ruthenium complex **11** proved to be highly efficient in the dehydrogenative oxidation of benzylic and primary alcohols, evidencing the potential of ligand **1**$^-$ as a powerful supporting ligand in organometallic catalysis. This work constitutes the first report of such a coordination mode for an anionic barbituric heterocycle and we are currently working on further implementations of this novel ligand structure in other metal/NHC-catalyzed reactions.

Scheme 4. Scope of the Ru-catalyzed dehydrogenative oxidation of primary alcohols by using pre-catalyst 11.[a]

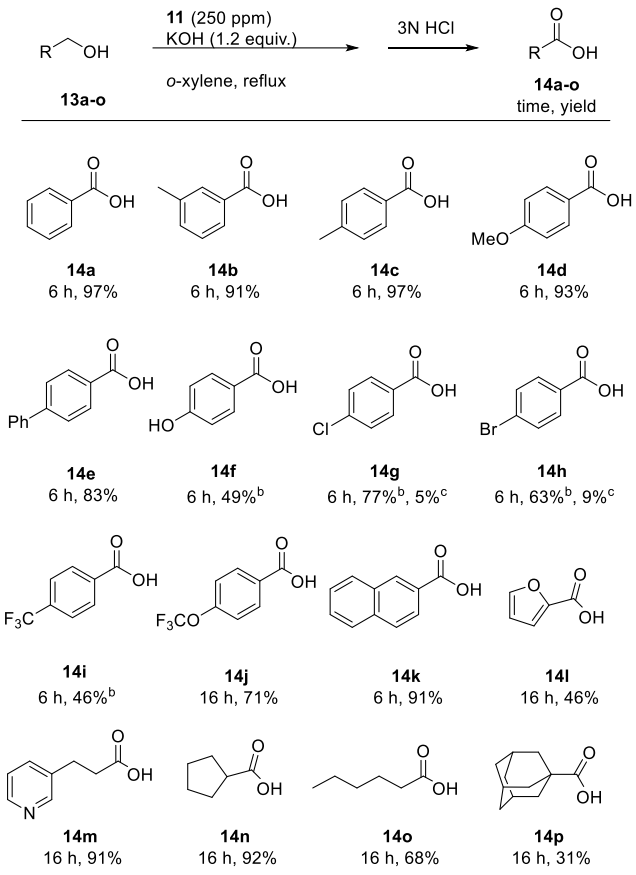

[a] Typical conditions: primary alcohol (3.75 mmol), potassium hydroxide (1.2 equiv), o-xylene (0.75 mL) and complex **11** (250 ppm) under air atmosphere; isolated yields. [b] 500 ppm catalyst used. [c] Yield of benzoic acid **14a.**

EXPERIMENTAL SECTION

General information

All manipulations were performed under an inert atmosphere of dry nitrogen for the syntheses or of dry argon for the catalytic tests by using standard vacuum line and Schlenk tube techniques. Dry and oxygen-free organic solvents (THF, Et_2O, CH_2Cl_2, toluene, pentane) were obtained using LabSolv (Innovative Technology) solvent purification system. [AuCl(tht)],[35] $[PdCl(C_3H_5)_2]_2$[36] and $[RhCl(1,5\text{-cod})]_2$,[37] and $[RhCl(nbd)]_2$[38] were synthesized according to literature procedures. All other reagent-grade chemicals were purchased from commercial sources and used as received. Chromatographic purification of the compounds was performed on silica gel (SiO_2, 40-63 µm or 60-200 µm) or deactivated aluminium oxide (neutral Al_2O_3, Brockmann type III (4.7% water), 50-200 µm). ^1H, ^{31}P, and ^{13}C NMR spectra were obtained on Bruker Avance 400, Avance III HD 400, or Avance 500 spectrometers and were referenced relative to the residual signals of the deuterated solvents (^1H and ^{13}C).[39] Chemical shifts were reported in ppm. ^1H and ^{13}C NMR signals were assigned by means of additional $^{13}C\{^1H,^{31}P\}$, ^{13}C-DEPT135, ^1H-^{13}C HMQC and/or HMBC experiments. Mass spectra (ESI mode) were obtained using a Xevo G2 QTof (Waters) spectrometer and were performed by the mass spectrometry service of the "Institut de chimie de Toulouse". Elemental analyses were carried out by the elemental analysis service of the LCC (Toulouse, France) using a Perkin Elmer 2400 series II analyzer.

[(η^3-allyl)[2-(2,6-diisopropylphenyl)-5-(1,3-diisopropyl-2,4,6-trioxo-hexahydropyrimidin-5-yl-κC^5)imidazo[1,5-*a*]pyridin-3-ylidene-κC^3]palladium(II)] (2)

n-BuLi (1.6 M in hexane, 268 µL, 0.43 mmol, 2.15 equiv) was added to a solution of HMDS (102 µL, 0.49 mmol, 2.45 equiv) in THF (3 mL) at room temperature. After 20 min, **1**·H (200 mg, 0.41 mmol, 2.05 equiv) was added. The mixture was stirred at room temperature for 20 min and solid $[PdCl(allyl)]_2$ (73 mg, 0.20 mmol, 1.0 equiv) was added at once. The solution was stirred overnight at room temperature and all volatiles were removed *in vacuo*. The residue was purified by flash chromatography (neutral Al_2O_3, Brockmann type III, CH_2Cl_2), washed with ether (5 mL) and dried to give a white solid (192 mg, 75%). Crystals suitable for an X-Ray diffraction experiment were grown by layering a solution of **2** in CH_2Cl_2 with pentane. ^1H NMR (400 MHz, $CDCl_3$): δ = 7.48 (t, *J* = 7.8 Hz, 1H, C*H* $_{p\text{-Dipp}}$), 7.30-7.19 (m, 3H, C*H* $_{Py}$ +C*H* $_{m\text{-Dipp}}$), 7.15 (s, 1H, C*H* $_{Im}$), 7.08 (dd, *J* = 9.2, 6.7 Hz, 1H, C*H* $_{Py}$), 6.64 (dd, *J* = 6.6, 0.9 Hz, 1H, C*H* $_{Py}$), 5.20 (hept, *J* = 6.9 Hz, 1H, NC*H*$(CH_3)_2$), 5.03 (hept, *J* = 6.9 Hz, 1H, NC*H*$(CH_3)_2$), 5.01-4.87 (m, 1H, C*H* $_{Allyl}$), 3.53 (dd, *J* = 7.4, 2.2 Hz, 1H, CH_2 $_{Allyl}$), 2.85 (d, *J* = 13.4 Hz, 1H, CH_2 $_{Allyl}$), 2.43 (hept, *J* = 6.8 Hz, 1H, C*H*$(CH_3)_2$), 2.43 (d, *J* = 6.9 Hz, 1H, CH_2 $_{Allyl}$), 2.11 (hept, *J* = 6.8 Hz, 1H, C*H*$(CH_3)_2$), 2.09-2.04 (m, 1H, CH_2 $_{Allyl}$), 1.48 (d, *J* = 6.9 Hz, 3H, NCH(CH_3)$_2$), 1.45 (d, *J* = 6.9 Hz, 3H, NCH(CH_3)$_2$), 1.38 (d, *J* = 6.9 Hz, 3H, NCH(CH_3)$_2$)), 1.35 (d, *J* = 6.9 Hz, 3H, NCH(CH_3)$_2$)), 1.13 (d, *J* = 6.9 Hz, 3H, CCH(CH_3)$_2$)), 1.10 (d, *J* = 6.l8 Hz, 3H, CCH(CH_3)$_2$)), 1.06 (d, *J* = 6.9 Hz, 3H, CCH(CH_3)$_2$)), 1.01 (d, *J* = 6.8 Hz, 3H, CCH(CH_3)$_2$)); $^{13}C\{^1H\}$ NMR (101 MHz, $CDCl_3$): δ = 170.7 (N_2C-Pd), 168.7 (*C*O), 165.8 (*C*O), 152.1 (*C*O), 146.2 (*C*$_{Ar}$), 145.5 (*C*$_{Ar}$), 141.4 (*C*$_{Py}$), 136.6 (*C*$_{Ar}$), 131.3 (*C*$_{Py}$), 130.3 (*CH*$_{p\text{-Dipp}}$), 126.9 (*C*H $_{Py}$), 123.8 (*C*H $_{m\text{-Dipp}}$), 123.6 (*C*H $_{m\text{-Dipp}}$), 116.9 (*C*H $_{allyl}$), 114.3 (*C*H $_{Py}$), 114.2 (*C*H $_{Py}$), 110.9 (*C*H $_{Im}$), 68.6 (*C*H_2 $_{allyl}$), 66.9 (Pd-*C*(CO)$_2$), 53.0 (*C*H_2 $_{allyl}$), 45.6 (N*C*H$(CH_3)_2$), 45.4 (N*C*H$(CH_3)_2$), 28.2 (C*C*H$(CH_3)_2$), 28.1 (C*C*H$(CH_3)_2$), 25.3 (CCH(*C*H_3)$_2$), 24.4 (CCH(*C*H_3)$_2$), 24.2 (CCH(*C*H_3)$_2$), 23.6 (CCH(*C*H_3)$_2$), 20.8 (NCH(*C*H_3)$_2$), 20.6 (NCH(*C*H_3)$_2$), 19.8 (NCH(*C*H_3)$_2$), 19.5 (NCH(*C*H_3)$_2$); MS (ESI^+): m/z (%): 635.2 (49) $[M + H]^+$ (*calcd* 635.2), 489.3 (100) [M – Pd – allyl +2H]$^+$ (*calcd* 489.3); Elemental analysis *calcd* (%) for $C_{32}H_{40}N_4O_3Pd$ (M_W = 635.11): C, 60.52; H, 6.35; N, 8.82; *found*: C, 60.52; H, 6.29; N, 8.71.

[(η^4-norbornadiene)[2-(2,6-diisopropylphenyl)-5-(1,3-diisopropyl-2,4,6-trioxo-hexahydropyrimidin-5-yl-κC^5)imidazo[1,5-*a*]pyridin-3-ylidene-κC^3]rhodium(I)] (3)

n-BuLi (1.6 M in hexane, 230 µL, 0.37 mmol, 1.2 equiv) was added to a solution of HMDS (90 µL, 0.37 mmol, 1.2 equiv) in THF (3 mL) at room temperature. After 20 min, **1**·H (150 mg, 0.31 mmol, 1.0 equiv) was added, and the mixture was stirred at room temperature for 20 min. Then $[RhCl(nbd)]_2$ (85 mg, 0.18 mmol, 0.6 equiv) was added all at once and the reaction mixture was stirred for 30 min. All volatiles were evaporated and the crude residue was washed with pentane (2×5 mL) to give an intense-orange solid (126 mg, 60%). Single crystals suitable for an X-Ray diffraction experiment were obtained by slow evaporation of a solution of **3** in pentane at room temperature. ^1H NMR (400 MHz, $CDCl_3$): δ = 7.42 (t, *J* = 7.8 Hz, 1H, C*H* $_{p\text{-Dipp}}$), 7.21 (d, *J* = 7.8 Hz, 2H, C*H* $_{m\text{-Dipp}}$), 7.11 (dd, *J* = 9.2, 0.9 Hz, 1H, C*H* $_{Py}$), 6.99 (dd, *J* = 9.2, 6.7 Hz, 1H, C*H* $_{Py}$), 6.89 (s, 1H, C*H* $_{Im}$), 6.54 (dd, *J* = 6.7, 0.9 Hz, 1H, C*H* $_{Py}$), 5.16 (hept, *J* = 6.9 Hz, 2H, NC*H*$(CH_3)_2$), 4.06-4.04 (m, 2H, C*H* $_{nbd}$), 3.58-3.55 (m, 2H, C*H* $_{nbd}$), 3.49-3.47 (m, 2H, C*H* $_{nbd}$), 2.40 (hept, *J* = 6.8Hz, 2H, CC*H*$(CH_3)_2$), 1.54 (d, *J* = 6.9 Hz, 6H, NCH(CH_3)$_2$), 1.48 (d, *J* = 6.9 Hz, 6H, NCH(CH_3)$_2$), 1.38 (d, *J* = 6.8 Hz, 6H, CCH(CH_3)$_2$)), 1.18-1.16 (m, 2H, CH_2 $_{nbd}$) 1.06 (d, *J* = 6.8 Hz, 6H, CCH(CH_3)$_2$)); $^{13}C\{^1H\}$ NMR (101 MHz, $CDCl_3$): δ = 166.8 (d, $^1J_{C\text{-}Rh}$ = 60.8 Hz, N_2C-Rh), 165.9 (N-*C*O), 152.0 (N_2*C*O), 145.8 (*C*$_{Dipp}$), 142.2 (d, $^2J_{C\text{-}Rh}$ = 1.7 Hz, *C* $_{Py}$), 134.6 (*C*$_{ipso\text{-}Dipp}$), 130.3 (*CH*$_{p\text{-}Dipp}$), 130.2 (d, $^3J_{C\text{-}Rh}$ =1.6 Hz, *C*$_{Py}$), 126.6 (*C*H$_{Py}$), 123.6 (*C*H$_{m\text{-}Dipp}$), 113.8 (*C*H$_{Py}$), 112.8 (*C*H$_{Py}$), 111.3 (*C*H$_{Im}$), 76.4 (d, $^1J_{C\text{-}Rh}$ = 6.8 Hz, *C*H$_{nbd}$), 69.8 (d, $^1J_{C\text{-}Rh}$ =14.3 Hz, Rh-*C*(CO)$_2$), 64.6 (d, $^1J_{C\text{-}Rh}$ = 5.1 Hz, *C*H_2 $_{nbd}$), 59.0 (d, $^1J_{C\text{-}Rh}$ = 10.4 Hz, *C*H$_{nbd}$), 52.1 (d, $^1J_{C\text{-}Rh}$ = 2.4 Hz, *C*H$_{nbd}$), 45.6 (N*C*H$(CH_3)_2$), 28.2

(C*C*H(CH$_3$)$_2$), 26.4 (CCH(*C*H$_3$)$_2$), 23.3 (CCH(*C*H$_3$)$_2$), 21.2 (NCH(*C*H$_3$)$_2$), 20.2 (NCH(*C*H$_3$)$_2$); MS (ESI$^+$): m/z (%): 715.2 (25) [M + H + MeOH]$^+$ (*calcd* 715.2), 682 (100) [M]$^+$ (*calcd* 682.2); Elemental analysis *calcd* (%) for $C_{36}H_{43}N_4O_3Rh$ (M_W = 682.67) + 0.3 CH_2Cl_2: C, 61.57.; H, 6.21; N, 7.91; *found*: C, 61.41; H, 6.38; N, 7.73 (*despite considerable drying under high vacuum, CH_2Cl_2 could not be removed in totality from the sample*).

[(η^4-1,5-cyclooctadiene)[2-(2,6-diisopropylphenyl)-5-(1,3-diisopropyl-2,4,6-trioxo-hexahydropyrimidin-5-yl-κ*C*^{5})imidazo[1,5-*a*]pyridin-3-ylidene-κ*C*^{3}]rhodium(I)] (4)

n-BuLi (1.6 M in hexane, 153 µL, 0.24 mmol, 1.2 equiv) was added to a solution of HMDS (60 µL, 0.29 mmol, 1.45 equiv) in THF (3 mL) at room temperature. The mixture was stirred for 20 min, and **1**·H (100 mg, 0.20 mmol, 1.0 equiv) was added as a solid. The solution was stirred at room temperature for 20 min, then [RhCl(COD)]$_2$ (50 mg, 0.10 mmol, 0.5 equiv) was added. After 1 hour, all volatiles were evaporated and the crude residue was purified by column chromatography (neutral Al_2O_3 Brockmann type III, CH_2Cl_2) and washed with pentane (5 mL) to give complex **4** as an orange powder (115 mg, 82 %). ^{1}H NMR (400 MHz, $CDCl_3$): δ = 7.45 (t, *J* = 7.8 Hz, 1H, C*H* $_{p\text{-Dipp}}$), 7.23 (d, *J* = 7.8 Hz, 2H, C*H* $_{m\text{-Dipp}}$), 7.10 (d *J* = 9.1 Hz, 1H, C*H* $_{Py}$), 6.96 (dd, *J* = 9.1, 6.7 Hz, 1H, C*H* $_{Py}$), 6.87 (s, 1H, C*H* $_{Im}$), 6.50 (d, *J* = 6.7 Hz, 1H, C*H* $_{Py}$), 5.16 (hept, *J* = 6.9 Hz, 2H, NC*H*(CH$_3$)$_2$), 4.13-4.07 (m, 2H, C*H* $_{COD}$), 3.81-3.75 (m, 2H, C*H* $_{COD}$), 2.48 (hept, *J* = 6.8Hz, 2H, CC*H*(CH$_3$)$_2$), 2.20-2.12 (m, 2H, C*H*$_2$ $_{COD}$), 2.02-1.93 (m, 2H, C*H*$_2$ $_{COD}$), 1.79-1.72 (m, 2H, C*H*$_2$ $_{COD}$), 1.64-1.57 (m, 2H, C*H*$_2$ $_{COD}$), 1.49 (d, *J* = 6.9 Hz, 6H, NCH(C*H*$_3$)$_2$), 1.47 (d, *J* = 6.9 Hz, 6H, NCH(C*H*$_3$)$_2$), 1.31 (d, *J* = 6.8 Hz, 6H, CCH(C*H*$_3$)$_2$)), 1.09 (d, *J* = 6.7 Hz, 6H, CCH(C*H*$_3$)$_2$)); ^{13}C{^{1}H} NMR (101 MHz, $CDCl_3$): δ = 167.8 (N-*C*O), 165.4 (d, $^1J_{C\text{-}Rh}$ = 55.2 Hz, N$_2$*C*-Rh), 151.8 (N$_2$*C*O), 145.7 (*C*$_{o\text{-Dipp}}$), 143.3 (*C*$_{Py}$), 135.0 (*C*$_{Dipp}$), 130.6 (*CH*$_{p\text{-Dipp}}$), 130.5 (*C*$_{Py}$), 126.4 (*C*H$_{Py}$), 124.0 (*C*H$_{m\text{-Dipp}}$), 113.6 (*C*H$_{Py}$), 112.2 (*C*H$_{Py}$), 112.1 (*C*H$_{Im}$), 93.7 (d, $^1J_{C\text{-}Rh}$ = 8.3 Hz, *C*H$_{COD}$), 75.5 (d, $^1J_{C\text{-}Rh}$ =11.9 Hz, *C*H$_{COD}$), 68.8 (d, $^1J_{C\text{-}Rh}$ =14.4 Hz, Rh-*C*(CO)$_2$), 45.5 (N*C*H(CH$_3$)$_2$), 31.4 (*C*H$_2$ $_{COD}$) , 29.6 (*C*H$_2$ $_{COD}$), 28.3 (C*C*H(CH$_3$)$_2$), 26.4 (CCH(*C*H$_3$)$_2$), 23.0 (CCH(*C*H$_3$)$_2$), 20.8 (NCH(*C*H$_3$)$_2$), 20.1 (NCH(*C*H$_3$)$_2$); MS (ESI$^+$): m/z (%): 1419.6 (100) [2M + Na]$^+$ (*calcd* 1419.5), 721.7 (54) [M + Na]$^+$ (*calcd* 723.3); Elemental analysis *calcd* (%) for $C_{37}H_{47}N_4O_3Rh$ (M_W = 698.71) + 0.5 H_2O: C, 62.79; H, 6.84; N, 7.92; *found*: C, 63.05; H, 6.61; N, 7.90 (water content in agreement with the integration of the ^{1}H NMR spectrum).

Dicarbonyl-[2-(2,6-diisopropylphenyl)-5-(1,3-diisopropyl-2,4,6-trioxo-hexahydropyrimidin-5-yl-κ*C*^{5})imidazo[1,5-*a*]pyridin-3-ylidene-κ*C*^{3}]rhodium(I) (5)

To a solution of **4** (57 mg, 0.08 mmol) in CH_2Cl_2 (2 mL) was bubbled gaseous carbon monoxide during 20 min, a color change from orange to yellow was observed. All volatiles were evaporated and the crude residue was washed with pentane (5 mL) to give complex **5** as a yellow powder (42 mg, 80 %). Single crystals suitable for an X-Ray diffraction experiment were obtained by crystallization from CH_2Cl_2/Et_2O/hexane at room temperature. ^{1}H NMR (400 MHz, $CDCl_3$): δ = 7.52 (t, *J* = 7.8 Hz, 1H, C*H* $_{p\text{-Dipp}}$), 7.31-7.29 (m, 3H, C*H*$_{m\text{-Dipp}}$ + C*H*$_{Py}$), 7.18-7.14 (m, 2H, C*H*$_{Py}$ + C*H*$_{Im}$), 6.65 (d, *J* = 6.8 Hz, 1H, C*H* $_{Py}$), 5.13 (hept, *J* = 7.1 Hz, 2H, NC*H*(CH$_3$)$_2$), 2.26 (hept, *J* = 7.0 Hz, 2H, CC*H*(CH$_3$)$_2$), 1.49 (d, *J* = 6.7 Hz, 6H, NCH(C*H*$_3$)$_2$), 1.48 (d, *J* = 6.6 Hz, 6H, NCH(C*H*$_3$)$_2$), 1.23 (d, *J* = 6.7 Hz, 6H, CCH(C*H*$_3$)$_2$)), 1.13 (d, *J* = 6.8 Hz, 6H, CCH(C*H*$_3$)$_2$)); ^{13}C{^{1}H} NMR (101 MHz, $CDCl_3$): δ = 189.0 (d, $^1J_{C\text{-}Rh}$ = 57.9 Hz, Rh-*C*O), 183.5 (d, $^1J_{C\text{-}Rh}$ = 68.2 Hz, Rh-*C*O), 170.2 (d, $^1J_{C\text{-}Rh}$ = 49.0 Hz, N$_2$*C*-Rh), 168.3 (d, $^2J_{C\text{-}Rh}$ = 1.8 Hz, N-*C*O), 151.4 (N$_2$*C*O), 146.1 (*C*$_{Dipp}$), 141.6 (*C*$_{Py}$), 135.3 (*C*$_{ipso\text{-Dipp}}$), 131.7 (*C*$_{Py}$), 131.1 (*CH*$_{p\text{-Dipp}}$), 127.5 (*C*H$_{Py}$), 124.3 (*C*H$_{m\text{-Dipp}}$), 114.5 (*C*H$_{Py}$), 114.4 (*C*H$_{Py}$), 111.8 (*C*H$_{Im}$), 67.3 (d, $^1J_{C\text{-}Rh}$ =15.8 Hz, Rh-*C*(CO)$_2$), 46.6 (N*C*H(CH$_3$)$_2$), 28.4 (C*C*H(CH$_3$)$_2$), 25.0 (CCH(*C*H$_3$)$_2$), 24.2 (CCH(*C*H$_3$)$_2$), 20.5 (NCH(*C*H$_3$)$_2$), 19.6 (NCH(*C*H$_3$)$_2$); IR (CH_2Cl_2): ν = 2069, 2010 cm^{-1} (C=O); MS (ESI$^+$): m/z (%): 673.2 (53) [M–2CO+2CH$_3$CN+H$^+$]$^+$ (*calcd* 673.2), 660.2 (100) [M–CO+CH$_3$CN+H$^+$]$^+$ (*calcd* 660.2), 619.2 (24) [M–CO+H$^+$]$^+$ (*calcd* 619.2); Elemental analysis *calcd* (%) for $C_{31}H_{35}N_4O_5Rh$ (M_W = 646.55) : C, 57.59; H, 5.46; N, 8.67; *found*: C, 57.62; H, 5.45; N, 8.30.

[(η^4-1,5-cyclooctadiene)[2-(2,6-diisopropylphenyl)-5-(1,3-diisopropyl-2,4,6-trioxo-hexahydropyrimidin-5-yl-κ*C*^{5})imidazo[1,5-*a*]pyridin-3-ylidene-κ*C*^{3}]iridium(I)] (6)

n-BuLi (1.6 M in hexane, 153 µL, 0.24 mmol, 1.2 equiv) was added to a solution of HMDS (60 µL, 0.29 mmol, 1.45 equiv) in THF (3 mL) at room temperature. After 20 min, **1**·H (100 mg, 0.20 mmol, 1.0 equiv) was added. The mixture was stirred at room temperature for 20 min, and [IrCl(COD)]$_2$ (68 mg, 0.10 mmol, 0.5 equiv) was added. All volatiles were evaporated and the crude residue was purified by column chromatography (neutral Al_2O_3 Brockmann type III, CH_2Cl_2) and washed with pentane (5 mL) to give complex **6** as a red powder (81 mg, 51 %). ^{1}H NMR (400 MHz, CD_2Cl_2): δ = 7.50 (t, *J* = 7.8 Hz, 1H, C*H* $_{p\text{-Dipp}}$), 7.28 (d, *J* = 7.8 Hz, 2H, C*H* $_{m\text{-Dipp}}$), 7.19 (dd, *J* = 9.1, 0.9 Hz, 1H, C*H* $_{Py}$), 7.05 (dd, *J* = 9.1, 6.7 Hz, 1H, C*H* $_{Py}$), 6.98 (s, 1H, C*H* $_{Im}$), 6.50 (dd, *J* = 6.7, 0.9 Hz, 1H, C*H* $_{Py}$), 5.08 (hept, *J* = 6.9 Hz, 2H, NC*H*(CH$_3$)$_2$), 3.81-3.79 (m, 2H, C*H* $_{COD}$), 3.41-3.39 (m, 2H, C*H* $_{COD}$), 2.51 (hept, *J* = 6.8 Hz, 2H, CC*H*(CH$_3$)$_2$), 2.03-1.93 (m, 2H, C*H*$_2$ $_{COD}$), 1.82-1.73 (m, 2H, C*H*$_2$ $_{COD}$), 1.62-1.57 (m, 2H, C*H*$_2$ $_{COD}$), 1.44 (d, *J* = 6.9 Hz, 6H, NCH(C*H*$_3$)$_2$), 1.43 (d, *J* = 6.9 Hz, 6H, NCH(C*H*$_3$)$_2$), 1.34-1.26 (m, 2H, C*H*$_2$ $_{COD}$), 1.29 (d, *J* = 6.8 Hz, 6H, CCH(C*H*$_3$)$_2$)), 1.10 (d, *J* = 6.8 Hz, 6H, CCH(C*H*$_3$)$_2$)); ^{13}C{^{1}H} NMR (101 MHz, CD_2Cl_2): δ = 168.2 (N-*C*O), 165.8 (N$_2$*C*-Ir), 152.0 (N$_2$*C*O), 146.2 (*C*$_{o\text{-Dipp}}$), 145.2 (*C*$_{Py}$), 135.5 (*C*$_{ipso\text{-Dipp}}$), 131.1 (*CH*$_{p\text{-Dipp}}$), 131.0 (*C*$_{Py}$), 126.9 (*C*H$_{Py}$), 124.5 (*C*H$_{m\text{-Dipp}}$), 114.5 (*C*H$_{Py}$), 114.0 (*C*H$_{Im}$), 112.4 (*C*H$_{Py}$), 80.1 (*C*H$_{COD}$), 70.6 (Ir-*C*(CO)$_2$), 61.5 (*C*H$_{COD}$), 46.2 (N*C*H(CH$_3$)$_2$), 32.5 (*C*H$_2$ $_{COD}$) , 30.9 (*C*H$_2$ $_{COD}$), 28.8 (C*C*H(CH$_3$)$_2$), 26.5 (CCH(*C*H$_3$)$_2$), 23.1 (CCH(*C*H$_3$)$_2$), 21.1 (NCH(*C*H$_3$)$_2$), 20.1 (NCH(*C*H$_3$)$_2$); MS (ESI$^+$): m/z (%): 789.3 (100) [M + H]$^+$ (*calcd* 789.3); HRMS (ESI$^+$): m/z *calcd*. for $C_{37}H_{48}N_4O_3Ir$: 789.3356; *found*: 789.3338, ε_r = 2.3 ppm. Complex **6** was assessed to be >98% pure by ^{1}H and ^{13}C NMR spectroscopy with main impurity being residual CH_2Cl_2 (see the Supporting Information).

[Chloro-[2-(2,6-diisopropylphenyl)-5-((1,3-diisopropyl-5-chloro-2,4,6-trioxo-hexahydropyrimidin-5-yl)imidazo[1,5-*a*]pyridin-3-ylidene]gold(I)] (9)

To a solution of HMDS (81 µL, 0.39 mmol, 1.4 equiv) in THF (5 mL) was added *n*-BuLi (1.6 M in hexane, 210 µL, 0.34 mmol, 1.2 equiv). The mixture was stirred at room temperature about 20 min. **1**·H (135 mg, 0.28 mmol) was added as a solid and the solution was stirred for 20 minutes at room temperature. After cooling to -50°C, [AuCl(tht)] (90 mg, 0.28 mmol, 1 equiv), was added all at once and the reaction mixture was allowed to warm up to room temperature over 5 hours in the cooling bath. All volatiles were evaporated and the crude mixture was taken up in CH_2Cl_2 (5 mL) and iodobenzene dichloride (152 mg, 0.55 mmol, 2.0 equiv) was added. After 20 min, the orange solution was evaporated and purified by column chromatography (neutral Al_2O_3, Brockmann's type 3, CH_2Cl_2). All volatiles were removed *in vacuo* and crystallization by slow evaporation of CH_2Cl_2 (2 mL) overnight at room temperature led to two types of crystals with two different colors, dark-green and orange crystals. After manual separation and X-Ray analysis, green crystals were attributed to compound **9**;[40] ^{1}H NMR (400 MHz,$CDCl_3$): δ = 7.72 (dd, *J* = 7.1, 1.2 Hz, 1H, C*H* $_{Py}$), 7.62 (dd, *J* = 9.2, 1.1 Hz, 1H, C*H* $_{Py}$), 7.49 (t, *J* = 7.8 Hz, 1H, C*H* $_{p\text{-Dipp}}$), 7.47 (s, 1H, C*H* $_{Im}$), 7.25-7.23 (m, 2H, C*H* $_{m\text{-Dipp}}$), 7.14 (dd, *J* = 9.2, 7.2 Hz, 1H, C*H* $_{Py}$), 5.04 (hept, *J* = 6.8 Hz, 2H, NC*H*(CH$_3$)$_2$), 2.10 (hept, *J* = 6.9 Hz, 2H, CC*H*(CH$_3$)$_2$), 1.59 (d, *J* = 6.9 Hz, 6H, NCH(C*H*$_3$)$_2$), 1.43 (d, *J* = 6.9 Hz, 6H, NCH(C*H*$_3$)$_2$), 1.24 (d, *J* = 6.8 Hz, 6H, CCH(C*H*$_3$)$_2$), 1.10 (d, *J* = 6.8 Hz, 6H, CCH(C*H*$_3$)$_2$); ^{13}C{^{1}H} NMR (101 MHz, $CDCl_3$): δ = 163.9 (N$_2$*C*), 162.6 (N-*C*O), 150.0 (N$_2$*C*O), 145.4 (*C* $_{o\text{-Dipp}}$), 135.0 (*C* $_{ipso\text{-Dipp}}$), 132.6 (*C* $_{Py}$), 131.2 (*C*H $_{p\text{-Dipp}}$), 129.7 (*C* $_{Py}$), 124.4 (*C*H $_{m\text{-Dipp}}$),122.9 (*C*H $_{Py}$), 122.1 (*C*H $_{Py}$), 120.1 (*C*H $_{Py}$), 114.3 (*C*H $_{Im}$), 64.2 (Cl-*C*(CO)$_2$), 50.0 (N*C*H(C*H*$_3$)$_2$), 28.6 (C*C*H(CH$_3$)$_2$), 24.6 (CCH(*C*H$_3$)$_2$), 24.1 (CCH(*C*H$_3$)$_2$), 19.9 (NCH(*C*H$_3$)$_2$), 18.5 (NCH(*C*H$_3$)$_2$).

[Dichloro-[[2-(2,6-diisopropylphenyl)-5(1,3-diisopropyl-2,4,6-trioxo-hexahydropyrimidin-5-yl-κ*C*^{5})imidazo[1,5-*a*]pyridin-3-ylidene-κ*C*^{3}]gold(III)] (10)

To a solution of HMDS (81 µL, 0.39 mmol, 1.4 equiv) in THF (5 mL) was added *n*-BuLi (1.6 M in hexane, 210 µL, 0.34 mmol, 1.2 equiv). The mixture was stirred at room temperature for 20 min. **1**·H (135 mg, 0.28 mmol, 1 equiv) was added as a solid and the solution was stirred for 20 minutes at room temperature. After cooling to -50°C, [AuCl(tht)] (90 mg, 0.28 mmol, 1 equiv), was added all at once and the reaction mixture was allowed to warm up to room temperature over 5 hours in the cooling bath. All volatiles were evaporated and the crude mixture was taken up in CH_2Cl_2 (5 mL) and iodobenzene dichloride (152 mg, 0.55 mmol, 2.0 equiv) was added. After 20 min, dichloromethane was evaporated and the residue was purified by column chromatography (neutral Al_2O_3, Brockmann's type 3, CH_2Cl_2) to afford a mixture of complexes **9** and **10**. In acetone-*d6*, based on the two singlets at δ_H 8.20 ppm and δ_H 8.35 ppm attributed respectively to the C*H*$_{Im}$ of the gold(III) complex **10** and C*H*$_{Im}$ of the gold(I) complex **9** protons, we were able to determine the ratio of the two gold complexes in the crude reaction mixture. The conversion of **9** to the thermodynamically more stable **10** occurred through successive crystallizations performed by slow evaporation of CH_2Cl_2 (2 mL) overnight at room temperature. The conversion was followed by ^{1}H NMR ($CDCl_3$) after each crystallization. The gold(III) complex **10** was obtained as an orange powder (151 mg, 72 %); ^{1}H NMR (400 MHz, $CDCl_3$): δ = 7.55 (t, *J* = 7.8 Hz, 1H, C*H* $_{p\text{-Dipp}}$), 7.47 (d, *J* = 9.2 Hz, 1H, C*H* $_{Py}$), 7.36 (s, 1H, C*H* $_{Im}$), 7.30-7.27 (m, 3H, C*H* $_{m\text{-Dipp}}$ + C*H* $_{Py}$), 6.73 (d, *J* = 6.8 Hz, 1H, C*H* $_{Py}$), 5.09 (hept, *J* = 6.7 Hz, 2H, NC*H*(CH$_3$)$_2$), 2.19 (hept, *J* = 6.9 Hz, 2H, CC*H*(CH$_3$)$_2$), 1.51 (d, *J* = 6.9 Hz, 6H, NCH(C*H*$_3$)$_2$), 1.48 (d, *J* = 6.9 Hz, 6H, NCH(C*H*$_3$)$_2$), 1.27 (d, *J* = 6.8 Hz, 6H, CCH(C*H*$_3$)$_2$), 1.13 (d, *J* = 6.8 Hz, 6H, CCH(C*H*$_3$)$_2$); ^{13}C NMR (101 MHz, $CDCl_3$): δ = 166.6 (N-*C*O-C), 150.5 (N$_2$*C*O), 145.0 (*C* $_{o\text{-Dipp}}$), 141.8 (N$_2$*C*), 138.6 (*C* $_{Py}$), 133.4 (*C* $_{ipso\text{-Dipp}}$), 131.5 (*C*H $_{p\text{-Dipp}}$), 130.5 (*C* $_{Py}$), 128.5 (*C*H $_{Py}$), 124.1 (*C*H $_{m\text{-Dipp}}$), 116.1 (*C*H $_{Py}$), 114.9 (*C*H $_{Py}$), 114.5 (*C*H $_{Im}$), 67.5 (Au-*C*(CO)$_2$), 48.3 (N*C*H(C*H*$_3$)$_2$), 28.9 (C*C*H(CH$_3$)$_2$), 25.1 (CCH(*C*H$_3$)$_2$), 23.6 (CCH(*C*H$_3$)$_2$), 20.4 (NCH(*C*H$_3$)$_2$), 19.3 (NCH(*C*H$_3$)$_2$); MS (ESI$^+$): m/z (%): 809.2 (100) [M + MeOH + Na]$^+$ (*calcd* 809.2), 772 (62) [M + H + NH$_3$]$^+$ (*calcd* 772.2), 760.2 (58) [M – Cl + CH$_3$CN]$^+$ (*calcd* 760.2), 719.2 (28) [M – Cl]$^+$ (*calcd* 719.2); HRMS (ESI$^+$): m/z *calcd*. for $C_{29}H_{39}AuCl_2N_5O_3$:772.2095; *found*: 772.2104, ε_r = 1.2 ppm; Elemental analysis *calcd* (%) for $C_{29}H_{35}AuCl_2N_4O_3$ (MW = 755.49) + 0.3 CH_2Cl_2: C 45.06, H 4.59, N 7.17; *found*: C 45.15, H 4.48, N 7.27 (*despite considerable drying under high vacuum, CH_2Cl_2 could not be removed in totality from the sample*).

[Chloro-(η^6-*p*-cymene)-[2-(2,6-diisopropylphenyl)-5-(1,3-diisopropyl-2,4,6-trioxo-hexahydropyrimidin-5-yl-κ*C*^{5})imidazo[1,5-*a*]pyridin-3-ylidene-κ*C*^{3}]ruthenium(II)] (11)

n-BuLi (2.5 M in hexane, 373 µL, 0.933 mmol, 1.25 equiv) was added to a solution of HMDS (218 µL, 1.05 mmol, 1.4 equiv) in THF (25 mL) at room temperature and the reaction mixture was stirred for 20 minutes. **1**·H (438 mg, 0.896 mmol, 1.2 equiv) was then added. The reaction mixture was stirred for another 20 minutes before the addition of [RuCl$_2$(*p*-cymene)]$_2$ (228 mg, 0.373 mmol, 0.5 equiv). The solution was stirred at room temperature overnight. The volatiles were removed under vacuum and the crude residue was purified by column chromatography (SiO_2, eluent DCM/MeOH: 95/5) to give complex **11** as a deep orange powder (435 mg, 77%). ^{1}H NMR (400 MHz, $CDCl_3$): δ = 7.59 (t, *J* = 7.7 Hz, 1H, C*H* $_{p\text{-Dipp}}$), 7.41 (dd, *J* = 11.4, 7.8 Hz, 2H, C*H* $_{m\text{-Dipp}}$), 7.13 (s, 1H, C*H* $_{Im}$), 7.03 (d, *J* = 9.1 Hz, 1H, C*H* $_{Py}$), 6.90 (dd, *J* = 9.2, 6.6 Hz, 1H, C*H* $_{Py}$), 6.31 (d, *J* = 6.6 Hz, 1H, C*H* $_{Py}$), 5.23 (hept, *J* = 6.9 Hz, 1H, NC*H*(CH$_3$)$_2$), 5.14 (br, 1H, C$_6$H$_4$ $_{p\text{-cym}}$), 5.06 (d, *J* = 5.9 Hz, 2H, C$_6$H$_4$ $_{p\text{-cym}}$), 4.85 (hept, *J* = 6.9 Hz, 1H, NC*H*(CH$_3$)$_2$), 4.43-4.87 (br, 1H, C$_6$H$_4$ $_{p\text{-cym}}$), 3.11 (hept, *J* = 6.6 Hz, 1H, CC*H*(CH$_3$)$_2$), 2.61-2.49 (m, 2H, CC*H*(CH$_3$)$_2$ + C$_6$H$_4$-C*H*(CH$_3$)$_2$), 1.75 (s, 3H, C*H*$_3$ $_{p\text{-cym}}$), 1.69 (d, *J* = 6.9 Hz, 3H, NCH(C*H*$_3$)$_2$), 1.55 (d, *J* = 6.9 Hz, 3H, NCH(C*H*$_3$)$_2$), 1.47 – 1.42 (m, 9H, NCH(C*H*$_3$)$_2$ + CCH(C*H*$_3$)$_2$), 1.23 (d, *J* = 6.6 Hz, 6H, CCH(C*H*$_3$)$_2$), 1.03 (d, *J* = 7.1 Hz, 6H, CCH(C*H*$_3$)$_2$), 0.88 (d, *J* = 7.1 Hz, 3H, CCH(C*H*$_3$)$_2$)); ^{13}C{^{1}H} NMR (101 MHz, $CDCl_3$): δ = 176.2 (N*C*O), 172.4 (N*C*O), 165.5 (N$_2$*C*-Ru), 152.3 (N$_2$*C*O), 148.7 (*C*$_{Dipp}$), 145.8 (*C*$_{Dipp}$), 143.5 (*C*$_{Py}$), 136.4 (*C*$_{Dipp}$), 131.0 (C$_{Py}$), 130.9 (*C*H $_{p\text{-Dipp}}$), 126.8 (*C*H$_{Py}$), 124.6 (*C*H $_{m\text{-Dipp}}$), 123.4 (*C*H $_{m\text{-Dipp}}$), 114.6 (*C*H$_{Py}$), 114.5 (*C*H$_{Im}$), 113.5 (*C*H$_{Py}$), 85.5 (C$_6$*H*$_4$), 80.1 (C$_6$*H*$_4$), 57.1 (Ru-*C*(CO)$_2$), 47.2 (N*C*H(CH$_3$)$_2$), 45.5 (N*C*H(CH$_3$)$_2$), 30.1 (*C*H(CH$_3$)$_2$), 28.6 (C*C*H(CH$_3$)$_2$), 28.0 ((C*C*H(CH$_3$)$_2$ + CCH(*C*H$_3$)$_2$), 26.9 (CCH(*C*H$_3$)$_2$), 23.0 (br, CCH(*C*H$_3$)$_2$), 22.0 (CCH(*C*H$_3$)$_2$), 22.5 (CCH(*C*H$_3$)$_2$), 21.9 (NCH(*C*H$_3$)$_2$), 21.5 (NCH(*C*H$_3$)$_2$), 21.2 (NCH(*C*H$_3$)$_2$), 20.6 (NCH(*C*H$_3$)$_2$), 19.9 (CCH(*C*H$_3$)$_2$), 16.7 (br, CH$_3$ $_{p\text{-cym}}$); MS (ESI$^+$): m/z (%): 781.2 (63) [M + Na]$^+$ (*calcd* 781.2); 759.3 (10) [M + H]$^+$ (*calcd* 759.3), 723.3 (100) [M - Cl]$^+$ (*calcd* 723.3); HRMS (ESI$^+$): m/z *calcd*. for $C_{39}H_{50}ClN_4O_3Ru$ ([M + H]$^+$): 759.2623; *found*: 759.2609, ε_r = 1.8 ppm. Complex **11** was assessed to be >99% pure by ^{1}H and ^{13}C NMR spectroscopy (see the Supporting Information).

[Tetracarbonyl-[2-(2,6-diisopropylphenyl)-5-(1,3-diisopropyl-2,4,6-trioxo-hexahydropyrimidin-5-yl-κ*C*^{5})imidazo[1,5-*a*]pyridin-3-ylidene-κ*C*^{3}]manganese(I)] (12)

n-BuLi (2.5 M in hexane, 196 µL, 0.49 mmol, 1.2 equiv) was added to a solution of HMDS (120 µL, 0.58 mmol, 1.4 equiv) in THF (3 mL) at room temperature. After 20 min, **1**·H (200 mg, 0.41 mmol, 1.0 equiv) was added. The mixture was stirred at room temperature for 20 min, and [MnBr(CO)$_5$] (114 mg, 0.41 mmol, 1.0 equiv) was added. After stirring overnight at 60°C, all volatiles were removed under vacuum. The crude mixture was purified by column chromatography (neutral Al_2O_3 Brockmann type III, toluene) under a nitrogen atmosphere, washed with pentane (5 mL) and dried to give complex **10** as a greenish powder (100 mg, 37 %). Single crystals suitable for X-Ray diffraction experiment were obtained by slow evaporation of a solution of complex **10** in $CHCl_3$. ^{1}H NMR (400 MHz, $CDCl_3$): δ = 7.51 (t, *J* = 7.7 Hz, 1H, C*H* $_{p\text{-Dipp}}$), 7.31 (d, *J* = 7.8 Hz, 2H, C*H* $_{m\text{-Dipp}}$), 7.33-7.22 (m, 2H, C*H* $_{Py}$ + C*H* $_{Im}$), 7.10-7.04 (m, 1H, C*H* $_{Py}$), 6.48 (d, *J* = 6.7 Hz, 1H, C*H* $_{Py}$), 5.16 (hept, *J* = 6.8 Hz, 2H, NC*H*(CH$_3$)$_2$), 2.36-2.31 (m, 2H, CC*H*(CH$_3$)$_2$), 1.51 (d, *J* = 6.8 Hz, 6H, NCH(C*H*$_3$)$_2$), 1.50 (d, *J* = 6.8 Hz, 6H, NCH(C*H*$_3$)$_2$), 1.26 (d, *J* = 6.8 Hz, 6H, CCH(C*H*$_3$)$_2$)), 1.09 (d, *J* = 6.8 Hz, 6H, CCH(C*H*$_3$)$_2$)); ^{13}C{^{1}H} NMR (101 MHz, $CDCl_3$): δ = 215.3 (Mn-*C*O), 214.2 (Mn-*C*O), 210.7 (Mn-*C*O), 173.7 (N-*C*O), 173.0 (N$_2$*C*-Mn), 151.0 (N$_2$*C*O), 146.1 (*C*$_{Dipp}$), 141.7 (*C*$_{Py}$), 135.0 (*C*$_{Dipp}$), 133.1 (*C*$_{Py}$), 131.2 (*C*H $_{p\text{-Dipp}}$), 126.8 (*C*H $_{Py}$), 124.2 (*C*H $_{m\text{-Dipp}}$), 116.0 (*C*H $_{Im}$), 115.1 (*C*H $_{Py}$), 114.6 (*C*H $_{Py}$), 60.6 (Mn-*C*(CO)$_2$) 46.4 (N*C*H(CH$_3$)$_2$), 28.4 (C*C*H(CH$_3$)$_2$), 26.8 (CCH(*C*H$_3$)$_2$), 22.5 (CCH(*C*H$_3$)$_2$), 20.4 (NCH(*C*H$_3$)$_2$), 19.6 (NCH(*C*H$_3$)$_2$); IR (CH_2Cl_2): ν = 2083, 2004, 1992, 1954, 1714, 1653 cm^{-1} (C=O); MS (ESI$^+$): m/z (%): 655.2 (18) [M + H]$^+$ (*calcd* 655.2), 649.2 (24) [M – CO + Na]$^+$ (*calcd* 649.2), 627.2 (100) [M – CO + H]$^+$ (*calcd* 627.2), 584.2 (90) [M – 4CO + CH$_3$CN + H]$^+$ (*calcd* 584.2), 575.2 (85) [M – 4 CO + MeOH + H]$^+$ (*calcd* 575.2), 543.2 (79) [M – 4 CO + H]$^+$ (*calcd* 543.2), 489.3 (48) [M – Mn(CO)$_4$ + H]$^+$ (*calcd* 489.3); HRMS (ESI$^+$): m/z *calcd*. for $C_{33}H_{36}N_4O_7Mn$: 655.1964; *found*: 655.1957, ε_r = 1.1 ppm. Complex **12** was assessed to be >98% pure by ^{1}H and ^{13}C NMR spectroscopy with main purity being residual CH_2Cl_2 (see the Supporting Information).

General screening procedure Ru-catalyzed dehydrogenative oxidation of primary alcohols

A stock solution of **11** (100 µL of a 9.3 mmol.L^{-1} solution in methylene chloride) was added to a Schlenk flask and methylene chloride was evaporated under high vacuum. Potassium hydroxide (1.2 equiv, 4.5 mmol, 252 mg), *o*-xylene (0.75 mL) and corresponding alcohol (3.75 mmol) were added, and a reflux condenser was set on top of the Schlenk flask. This latter was subsequently placed in a preheated oil bath at 150 °C. The mixture was stirred under reflux for 6 or 16 hours. The reaction mixture was cooled down to room temperature, water (4 mL) was added and the reaction mixture was stirred for additional 10 min. and sonicated if required to dissolve the carboxylate salt. The aqueous layer was then extracted with diethyl ether (3 x 20 mL) to remove unreacted alcohol. The water layer was acidified to pH = 2 using a 3N HCl solution and the carboxylic acid product was extracted with ethyl acetate (3 x 20 mL). The combined organic layers were dried over sodium sulfate, concentrated and dried under vacuum. Carboxylic acid

14f-i were purified Flash column chromatography (CombiFlash, SiO_2, *n*-hexane/ethyl acetate gradient from 10 to 40 % as eluent).

Crystal Structure Determination

The crystals were kept in their mother liquor until they were dipped in perfluoropolyether oil and their structure determined. The chosen crystals were mounted on a MiTeGen MicroMount and quickly cooled down to either 100 K. The selected crystals were mounted on a Bruker Kappa APEX II using a micro-focus molybdenum Kα radiation (λ= 0.71073 Å) with a graphite monochromator and equipped with an Oxford Cryosystems Cooler Device. The unit cell determination and data integration were carried out using APEXII[41]. The structures have been solved by Direct Methods using SHELXS,[42] and refined by least-squares procedures with SHELXL[43] included in the software packages WinGX version 1.63.[42] Atomic Scattering Factors were taken from the International Tables for X-Ray Crystallography.[44] Absorption correction was done using multi-scan DENZO/SCALEPACK (Otwinowski & Minor, 1997) method.[45] All hydrogen atoms were geometrically placed and refined using a riding model.

All non-hydrogen atoms were anisotropically refined. Details of the structure solution and refinements are given in the Supporting Information (CIF file).

ASSOCIATED CONTENT

Supporting Information

The Supporting Information is available free of charge on the ACS Publications website.

NMR spectra and characterization of the products of catalysis (PDF)
Crystallographic data (CIF)

Accession Codes

CCDC 2085777-2085784 contain the supplementary crystallographic data for this paper. These data can be obtained free of charge via www.ccdc.cam.ac.uk/data_request/cif, or by emailing data_request@ccdc.cam.ac.uk, or by contacting The Cambridge Crystallographic Data Centre, 12 Union Road, Cambridge CB2 1EZ, UK; fax: +44 1223 336033.

AUTHOR INFORMATION

Corresponding Author

* E-mail for V.C.: vincent.cesar@lcc-toulouse.fr
* E-mail for S.B.: stephanie.bastin@lcc-toulouse.fr

Notes

The authors declare no competing financial interest.

ACKNOWLEDGMENT

This work was supported by the Agence Nationale de la Recherche (ANR-16-CE07-0006), the Centre National de la Recherche Scientifique (CNRS) and the University Côte d'Azur. I.B. is grateful to ANR for PhD grants and K.G. to the French government for part of a PhD grant.

REFERENCES

(1) (a) Hopkinson, M. N.; Richter, C.; Schedler, M.; Glorius, F. An overview of N-heterocyclic carbenes. *Nature* **2014**, *510*, 485-496; (b) Munz, D. Pushing Electrons—Which Carbene Ligand for Which Application? *Organometallics* **2018**, *37*, 275-289; (c) Hahn, F. E.; Jahnke, M. C. Heterocyclic Carbenes: Synthesis and Coordination Chemistry. *Angew. Chem. Int. Ed.* **2008**, *47*, 3122-3172.

(2) Díez-González, S. N-Heterocyclic Carbenes: From Laboratory Curiosities to Efficient Synthetic Tools, 2nd ed.; RSC: Cambridge, U.K., 2017

(3) Benhamou, L.; Chardon, E.; Lavigne, G.; Bellemin-Laponnaz, S.; César, V. Synthetic Routes to N-Heterocyclic Carbene Precursors. *Chem. Rev.* **2011**, *111*, 2705-2733.

(4) (a) Huynh, H. V. Electronic Properties of N-Heterocyclic Carbenes and Their Experimental Determination. *Chem. Rev.* **2018**, *118*, 9457-9492; (b) Gomez-Suarez, A.; Nelson, D. J.; Nolan, S. P. Quantifying and understanding the steric properties of N-heterocyclic carbenes. *Chem. Commun.* **2017**, *53*, 2650-2660.

(5) (a) Peris, E. Smart N-Heterocyclic Carbene Ligands in Catalysis. *Chem. Rev.* **2018**, *118*, 9988-10031; (b) Bellemin-Laponnaz, S.; Dagorne, S. Group 1 and 2 and Early Transition Metal Complexes Bearing N-Heterocyclic Carbene Ligands: Coordination Chemistry, Reactivity, and Applications. *Chem. Rev.* **2014**, *114*, 8747-8774; (c) Liang, Q.; Song, D. Iron N-heterocyclic carbene complexes in homogeneous catalysis. *Chem. Soc. Rev.* **2020**, *49*, 1209-1232; (d) Ogba, O. M.; Warner, N. C.; O'Leary, D. J.; Grubbs, R. H. Recent advances in ruthenium-based olefin metathesis. *Chem. Soc. Rev.* **2018**, *47*, 4510-4544; (e) Froese, R. D. J.; Lombardi, C.; Pompeo, M.; Rucker, R. P.; Organ, M. G. Designing Pd–N-Heterocyclic Carbene Complexes for High Reactivity and Selectivity for Cross-Coupling Applications. *Acc. Chem. Res.* **2017**, *50*, 2244-2253; (f) Zhao, Q.; Meng, G.; Nolan, S. P.; Szostak, M. N-Heterocyclic Carbene Complexes in C–H Activation Reactions. *Chem. Rev.* **2020**, *120*, 1981-2048.

(6) (a) Smith, C. A.; Narouz, M. R.; Lummis, P. A.; Singh, I.; Nazemi, A.; Li, C.-H.; Crudden, C. M. N-Heterocyclic Carbenes in Materials Chemistry. *Chem. Rev.* **2019**, *119*, 4986-5056; (b) Strassner, T. Phosphorescent Platinum(II) Complexes with C∧C* Cyclometalated NHC Ligands. *Acc. Chem. Res.* **2016**, *49*, 2680-2689.

(7) Mora, M.; Gimeno, M. C.; Visbal, R. Recent advances in gold–NHC complexes with biological properties. *Chem. Soc. Rev.* **2019**, *48*, 447-462.

(8) M-NHC bonds can nevertheless react under certain conditions, please see: Chernyshev, V. M.; Denisova, E. A.; Eremin, D. B.; Ananikov, V. P. The key role of R–NHC coupling (R = C, H, heteroatom) and M–NHC bond cleavage in the evolution of M/NHC complexes and formation of catalytically active species. *Chem. Sci*. **2020**, *11*, 6957-6977.

(9) (a) Hoveyda, A. H.; Zhou, Y.; Shi, Y.; Brown, M. K.; Wu, H.; Torker, S. Sulfonate N-Heterocyclic Carbene–Copper Complexes: Uniquely Effective Catalysts for Enantioselective Synthesis of C−C, C−B, C−H, and C−Si Bonds. *Angew. Chem. Int. Ed.* **2020**, *59*, 21304-21359; (b) Fliedel, C.; Labande, A.; Manoury, E.; Poli, R. Chiral N-heterocyclic carbene ligands with additional chelating group(s) applied to homogeneous metal-mediated asymmetric catalysis. *Coord. Chem. Rev.* **2019**, *394*, 65-103; (c) Hameury, S.; de Fremont, P.; Braunstein, P. Metal complexes with oxygen-functionalized NHC ligands: synthesis and applications. *Chem. Soc. Rev.* **2017**, *46*, 632-733; (d) Charra, V.; de Frémont, P.; Braunstein, P. Multidentate N-heterocyclic carbene complexes of the 3d metals: Synthesis, structure, reactivity and catalysis. *Coord. Chem. Rev.* **2017**, *341*, 53-176.

(10) Poyatos, M.; Mata, J. A.; Peris, E. Complexes with Poly(N-heterocyclic carbene) Ligands: Structural Features and Catalytic Applications. *Chem. Rev.* **2009**, *109*, 3677-3707.

(11) Mo, Z.; Chen, D.; Leng, X.; Deng, L. Intramolecular C(sp3)–H Bond Activation Reactions of Low-Valent Cobalt Complexes with Coordination Unsaturation. *Organometallics* **2012**, *31*, 7040-7043.

(12) Scott, N. M.; Dorta, R.; Stevens, E. D.; Correa, A.; Cavallo, L.; Nolan, S. P. Interaction of a Bulky N-Heterocyclic Carbene Ligand with Rh(I) and Ir(I). Double C−H Activation and Isolation of Bare 14-Electron Rh(III) and Ir(III) Complexes. *J. Am. Chem. Soc.* **2005**, *127*, 3516-3526.

(13) Herbert, M. B.; Grubbs, R. H. Z-Selective Cross Metathesis with Ruthenium Catalysts: Synthetic Applications and Mechanistic Implications. *Angew. Chem. Int. Ed.* **2015**, *54*, 5018-5024.

(14) Kruger, A.; Neels, A.; Albrecht, M. Rhodium-mediated activation of an alkane-type C-H bond. *Chem. Commun.* **2010**, *46*, 315-317.

(15) (a) Sun, J.; Ou, C.; Wang, C.; Uchiyama, M.; Deng, L. Silane-Functionalized N-Heterocyclic Carbene–Cobalt Complexes Containing a Five-Coordinate Silicon with a Covalent Co–Si Bond. *Organometallics* **2015**, *34*, 1546-1551; (b) Ríos, P.; Fouilloux, H.;

Díez, J.; Vidossich, P.; Lledós, A.; Conejero, S. σ-Silane Platinum(II) Complexes as Intermediates in C−Si Bond-Coupling Processes. *Chem. Eur. J.* **2019**, *25*, 11346-11355; (c) Paul, D.; Beiring, B.; Plois, M.; Ortega, N.; Kock, S.; Schlüns, D.; Neugebauer, J.; Wolf, R.; Glorius, F. A Cyclometalated Ruthenium-NHC Precatalyst for the Asymmetric Hydrogenation of (Hetero)arenes and Its Activation Pathway. *Organometallics* **2016**, *35*, 3641-3646.
(16) (a) Barthes, C.; Bijani, C.; Lugan, N.; Canac, Y. A Palladium(II) Complex of a C4 Chelating Bis(NHC) Diphosphonium Bis(ylide) Ligand. *Organometallics* **2018**, *37*, 673-678; (b) Benaissa, I.; Taakili, R.; Lugan, N.; Canac, Y. A convenient access to N-phosphonio-substituted NHC metal complexes [M = Ag(i), Rh(i), Pd(ii)]. *Dalton Trans.* **2017**, *46*, 12293-12305.
(17) (a) Benhamou, L.; Bastin, S.; Lugan, N.; Lavigne, G.; César, V. Metal-assisted conversion of an N-ylide mesomeric betaine into its carbenic tautomer: generation of N-(fluoren-9-yl)imidazol-2-ylidene complexes. *Dalton Trans.* **2014**, *43*, 4474-4482; (b) Downing, S. P.; Pogorzelec, P. J.; Danopoulos, A. A.; Cole-Hamilton, D. J. Indenyl- and Fluorenyl-Functionalized N-Heterocyclic Carbene Complexes of Rhodium and Iridium – Synthetic, Structural and Catalytic Studies. *Eur. J. Inorg. Chem.* **2009**, *2009*, 1816-1824.
(18) Oertel, A. M.; Freudenreich, J.; Gein, J.; Ritleng, V.; Veiros, L. F.; Chetcuti, M. J. Intramolecular Nitrile C–H Bond Activation in Nickel NHC Complexes: A Route to New Nickelacycles. *Organometallics* **2011**, *30*, 3400-3411.
(19) (a) Azouzi, K.; Duhayon, C.; Benaissa, I.; Lugan, N.; Canac, Y.; Bastin, S.; César, V. Bidentate Iminophosphorane-NHC Ligand Derived from the Imidazo[1,5-a]pyridin-3-ylidene Scaffold. *Organometallics* **2018**, *37*, 4726-4735; (b) Zhang, Y.; Lavigne, G.; Lugan, N.; César, V. Buttressing Effect as a Key Design Principle towards Highly Efficient Palladium/N-Heterocyclic Carbene Buchwald–Hartwig Amination Catalysts. *Chem. Eur. J.* **2017**, *23*, 13792-13801.
(20) (a) Reshi, N. U. D.; Bera, J. K. Recent advances in annellated NHCs and their metal complexes. *Coord. Chem. Rev.* **2020**, *422*, 213334; (b) Iglesias-Siguenza, J.; Izquierdo, C.; Diez, E.; Fernandez, R.; Lassaletta, J. M. Chirality and catalysis with aromatic N-fused heterobicyclic carbenes. *Dalton Trans.* **2016**, *45*, 10113-10117.
(21) Tang, Y.; Benaissa, I.; Huynh, M.; Vendier, L.; Lugan, N.; Bastin, S.; Belmont, P.; César, V.; Michelet, V. An Original L-shape, Tunable N-Heterocyclic Carbene Platform for Efficient Gold(I) Catalysis. *Angew. Chem. Int. Ed.* **2019**, *58*, 7977-7981.
(22) (a) Chan, W.-W.; Lo, S.-F.; Zhou, Z.; Yu, W.-Y. Rh-Catalyzed Intermolecular Carbenoid Functionalization of Aromatic C–H Bonds by α-Diazomalonates. *J. Am. Chem. Soc.* **2012**, *134*, 13565-13568; (b) Gaillard, S.; Slawin, A. M. Z.; Nolan, S. P. A N-Heterocyclic Carbene Gold Hydroxide Complex: a Golden Synthon. *Chem. Commun.* **2010**, *46*, 2742-2744; (c) Stow, C. P.; Widenhoefer, R. A. Synthesis, Structure, and Reactivity of Gold(I) α-Oxo Carbenoid Complexes. *Organometallics* **2020**, *39*, 1249-1257; (d) Kawato, T.; Uechi, T.; Koyama, H.; Kanatomi, H.; Kawanami, Y. Preparation, Structure, and Properties of Central-Carbon-Bonded Diethyl Malonato Complexes of Palladium(II) with Bis-(μ-Chloro) and μ-Oxalato Bridges. *Inorg. Chem.* **1984**, *23*, 764-769.
(23) Noguchi, K.; Tamura, T.; Yuge, H.; Miyamoto, T. K. Linkage Isomerism of Organoplatinum(II) Compounds Coordinated by two 1,3-Dimethylbarbiturate Anions. *Acta Cryst.* **2000**, *C56*, 171-173.
(24) (a) Newkome, G. R.; Evans, D. W. A Route to Thermally Stable Organonickel(II) Complexes Containing two Csp3-Ni(II) Bonds *ARKIVOC* **2002**, *viii*, 40-45; (b) Newkome, G. R.; Evans, D. W.; Kiefer, G. E.; Theriot, K. J. Metallocyclic Complexes of Palladium(II) and Platinum(II) Containing Six- and Seven-Membered Chelate Rings. *Organometallics* **1988**, *7*, 2537-2542; (c) Newkome, G. R.; Gupta, V. K.; Fronczek, F. R. Palladium(II) Complexes of Pyridine- and Pyrazine-Based Ligands with trans Bis(Carbon-Metal) Bonds. Ligand Synthesis, Complexation, and Crystal Structure. *Organometallics* **1982**, *1*, 907-910.
(25) Alcarazo, M.; Roseblade, S. J.; Cowley, A. R.; Fernández, R.; Brown, J. M.; Lassaletta, J. M. Imidazo[1,5-a]pyridine: A Versatile Architecture for Stable N-Heterocyclic Carbenes. *J. Am. Chem. Soc.* **2005**, *127*, 3290-3291.
(26) Roseblade, S. J.; Ros, A.; Monge, D.; Alcarazo, M.; Álvarez, E.; Lassaletta, J. M.; Fernández, R. Imidazo[1,5-a]pyridin-3-ylidene/Thioether Mixed C/S Ligands and Complexes Thereof. *Organometallics* **2007**, *26*, 2570-2578.
(27) César, V.; Labat, S.; Miqueu, K.; Sotiropoulos, J.-M.; Brousses, R.; Lugan, N.; Lavigne, G. The Ambivalent Chemistry of a Free Anionic N-Heterocyclic Carbene Decorated with a Malonate Backbone: The Plus of a Negative Charge. *Chem. Eur. J.* **2013**, *19*, 17113-17124.
(28) (a) Taakili, R.; Lepetit, C.; Duhayon, C.; Valyaev, D. A.; Lugan, N.; Canac, Y. Palladium(ii) pincer complexes of a C,C,C-NHC, diphosphonium bis(ylide) ligand. *Dalton Trans.* **2019**, *48*, 1709-1721; (b) Iwai, T.; Tanaka, R.; Sawamura, M. Synthesis, Coordination Properties, and Catalytic Application of Triarylmethane-Monophosphines. *Organometallics* **2016**, *35*, 3959-3969.
(29) Leung, C. H.; Incarvito, C. D.; Crabtree, R. H. Interplay of Linker, N-Substituent, and Counterion Effects in the Formation and Geometrical Distortion of N-Heterocyclic Biscarbene Complexes of Rhodium(I). *Organometallics* **2006**, *25*, 6099-6107.
(30) Canac, Y.; Lepetit, C.; Abdalilah, M.; Duhayon, C.; Chauvin, R. Diaminocarbene and Phosphonium Ylide Ligands: A Systematic Comparison of their Donor Character. *J. Am. Chem. Soc.* **2008**, *130*, 8406-8413.
(31) (a) Shiotani, A.; Schmidbaur, H. Organogold-chemie IX. Versuche zur Oxydativen Addition an Organogold-Komplexen. *J. Organomet. Chem.* **1972**, *37*, C24-C26; (b) Tamaki, A.; Kochi, J. K. Catalytic mechanism involving oxidative addition in the coupling of alkylgold(I) with alkyl halides. *J. Organomet. Chem.* **1972**, *40*, C81-C84.
(32) (a) Santilli, C.; Makarov, I. S.; Fristrup, P.; Madsen, R. Dehydrogenative Synthesis of Carboxylic Acids from Primary Alcohols and Hydroxide Catalyzed by a Ruthenium N-Heterocyclic Carbene Complex. *J. Org. Chem.* **2016**, *81*, 9931-9938; (b) Malineni, J.; Keul, H.; Möller, M. A green and sustainable phosphine-free NHC-ruthenium catalyst for selective oxidation of alcohols to carboxylic acids in water. *Dalton Trans.* **2015**, *44*, 17409-17414.
(33) Wang, Z.-Q.; Tang, X.-S.; Yang, Z.-Q.; Yu, B.-Y.; Wang, H.-J.; Sang, W.; Yuan, Y.; Chen, C.; Verpoort, F. Highly active bidentate N-heterocyclic carbene/ruthenium complexes performing dehydrogenative coupling of alcohols and hydroxides in open air. *Chem. Commun.* **2019**, *55*, 8591-8594.
(34) (a) Kim, S. M.; Shin, H. Y.; Kim, D. W.; Yang, J. W. Metal-Free Chemoselective Oxidative Dehomologation or Direct Oxidation of Alcohols: Implication for Biomass Conversion. *ChemSusChem* **2016**, *9*, 241-245; (b) Wang, J.; Liu, C.; Yuan, J.; Lei, A. Transition-metal-free aerobic oxidation of primary alcohols to carboxylic acids. *New J. Chem.* **2013**, *37*, 1700-1703.
(35) Hashmi, A. S. K.; Hengst, T.; Lothschütz, C.; Rominger, F. New and Easily Accessible Nitrogen Acyclic Gold(I) Carbenes: Structure and Application in the Gold-Catalyzed Phenol Synthesis as well as the Hydration of Alkynes. *Adv. Synth. Catal.* **2010**, *352*, 1315-1337.
(36) Marion, N.; Navarro, O.; Mei, J.; Stevens, E. D.; Scott, N. M.; Nolan, S. P. Modified (NHC)Pd(allyl)Cl (NHC = N-Heterocyclic Carbene) Complexes for Room-Temperature Suzuki−Miyaura and Buchwald−Hartwig Reactions. *J. Am. Chem. Soc.* **2006**, *128*, 4101-4111.
(37) Giordiano, G. C., R. H.; Heinz, R.M.; Forster, D.; Morris, D.E., Di-μ-chloro-bis-(η4-1,5-cyclooctadiene)-dirhodium(I). In *Inorganic Syntheses: Reagents for Transition Metal Complex and Organometallic Syntheses*, Angelici, R. J., Ed. Wiley and Sons, Inc: 1990; Vol. 28, p 88.
(38) Abel, E. W.; Bennett, M. A.; Wilkinson, G. Norbornadiene–Metal Complexes and some Related Compounds. *J. Chem. Soc.* **1959**, 3178-3182.
(39) Fulmer, G. R.; Miller, A. J. M.; Sherden, N. H.; Gottlieb, H. E.; Nudelman, A.; Stoltz, B. M.; Bercaw, J. E.; Goldberg, K. I. NMR Chemical Shifts of Trace Impurities: Common Laboratory Solvents, Organics, and Gases in Deuterated Solvents Relevant to the Organometallic Chemist. *Organometallics* **2010**, *29*, 2176-2179.
(40) The isolated yield of complex 9 is not given as it varies with the time taken to crystallise the mixture of complex 9 and 10.
(41) SAINT Bruker. Bruker AXS Inc., Madison, Wisconsin, USA. **2007**.
(42) Farrugia, L. WinGX suite for small-molecule single-crystal crystallography. *J. Appl. Cryst.* **1999**, *32*, 837-838.
(43) Sheldrick, G. A short history of SHELX. *Acta Cryst.* **2008**, *A64*, 112-122.
(44) INTERNATIONAL tables for X-Ray crystallography, 1974, Vol IV, Kynoch press, Birmingham, England

(45) Blessing, R. An empirical correction for absorption anisotropy.
Acta Cryst. **1995**, *A51*, 33-38.